CoMP linear polarization as a probe of coronal magnetic topology

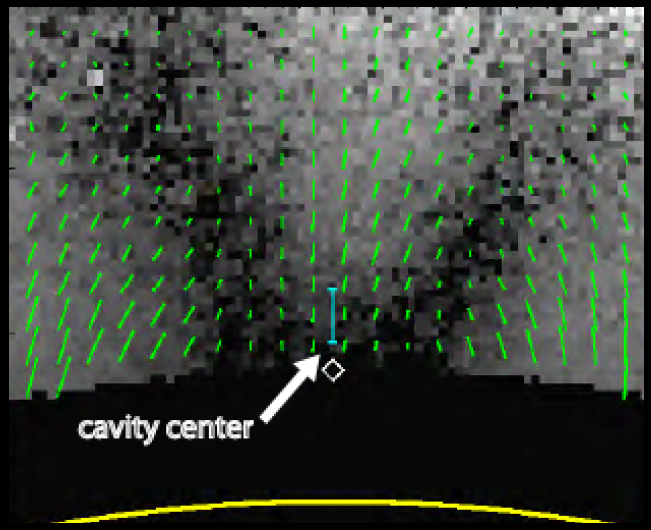

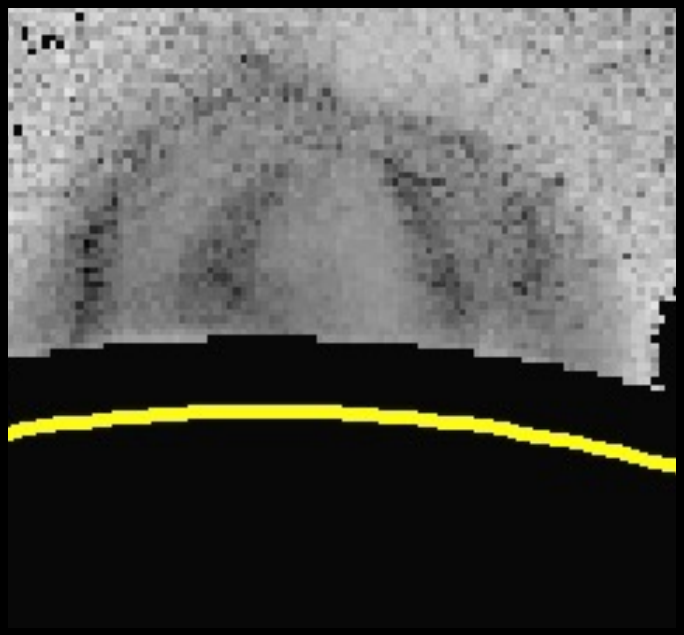

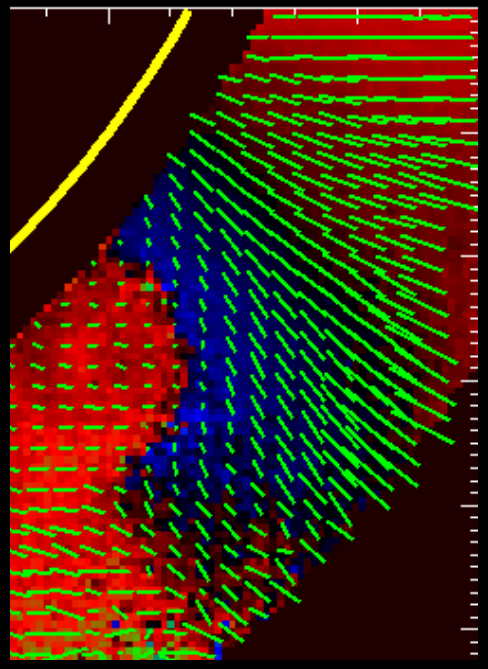

Sarah Gibson, Urszula Bak-Steslicka, Giuliana de Toma, Laurel Rachmeler, Mei Zhang

Thanks to Yuhong Fan and Cooper Downs

CoMP linear polarization as a probe of coronal magnetic topology

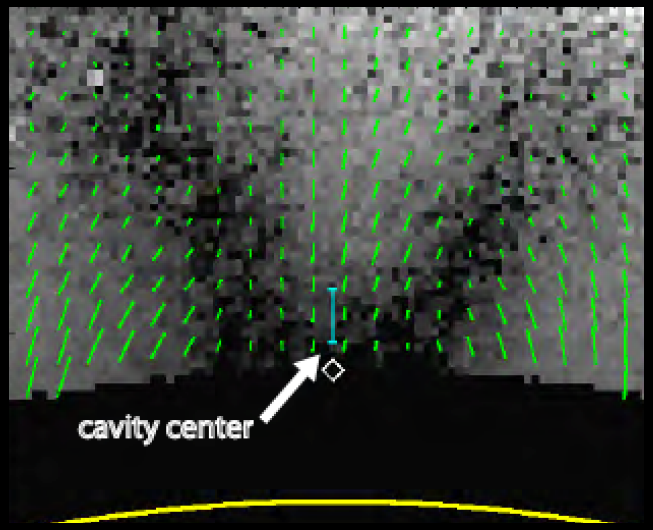

Lagomorphs

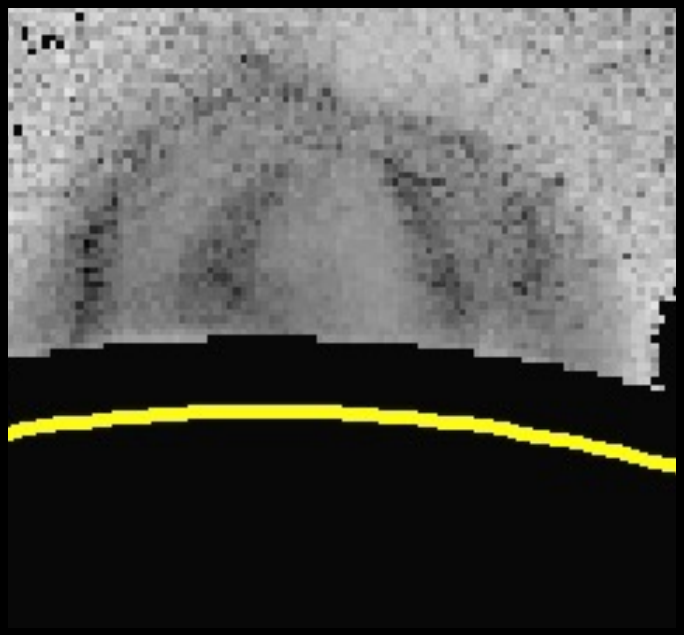

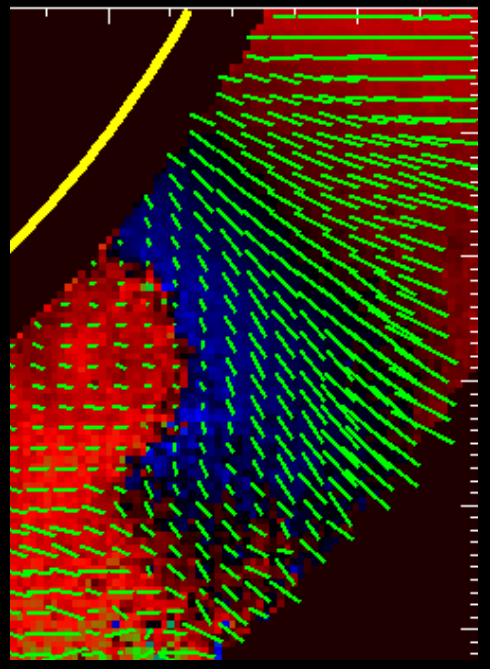

Sarah Gibson, Urszula Bak-Steslicka, Giuliana de Toma, Laurel Rachmeler, Mei Zhang

Thanks to Yuhong Fan and Cooper Downs

CoMP linear polarization as a probe of coronal magnetic topology

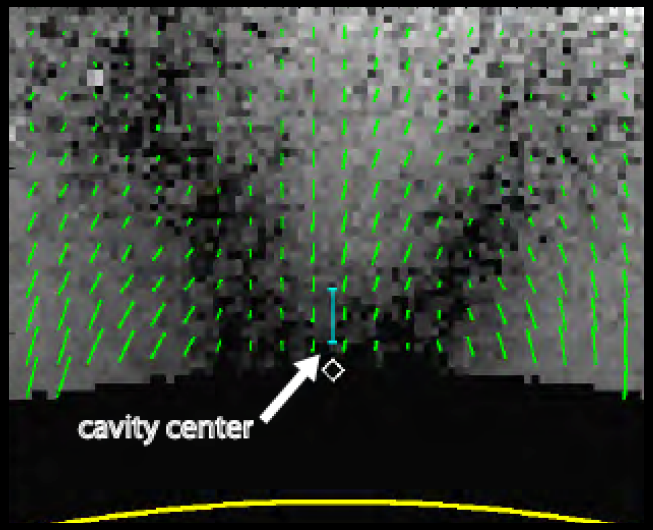

Lagomorphs

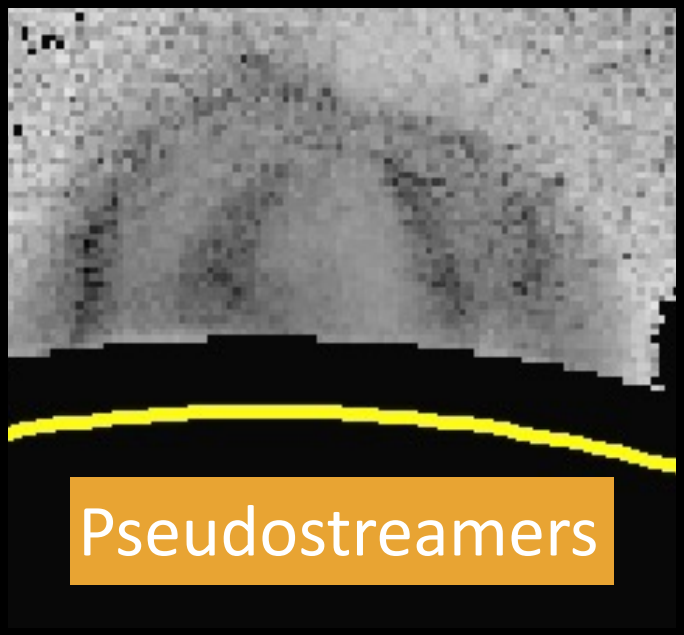

Pseudostreamers

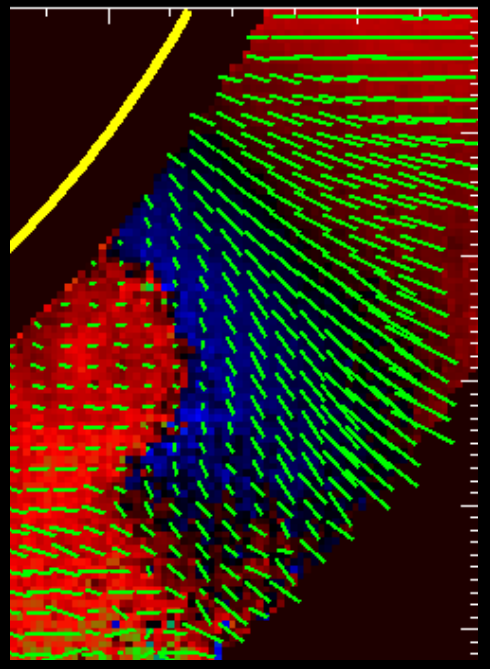

Sarah Gibson, Urszula Bak-Steslicka, Giuliana de Toma, Laurel Rachmeler, Mei Zhang

Thanks to Yuhong Fan and Cooper Downs

CoMP linear polarization as a probe of coronal magnetic topology

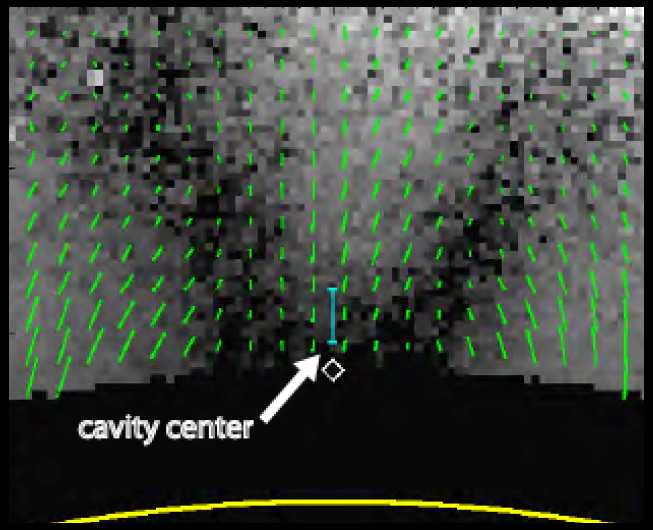

Lagomorphs

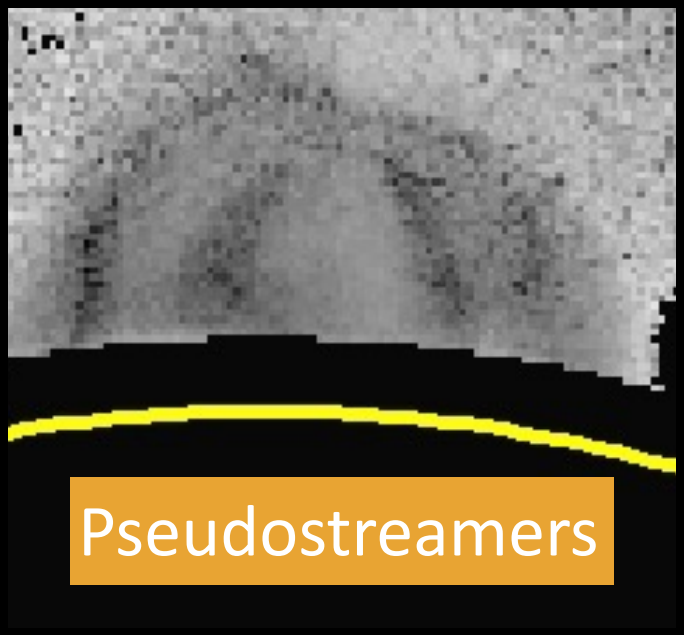

Pseudostreamers

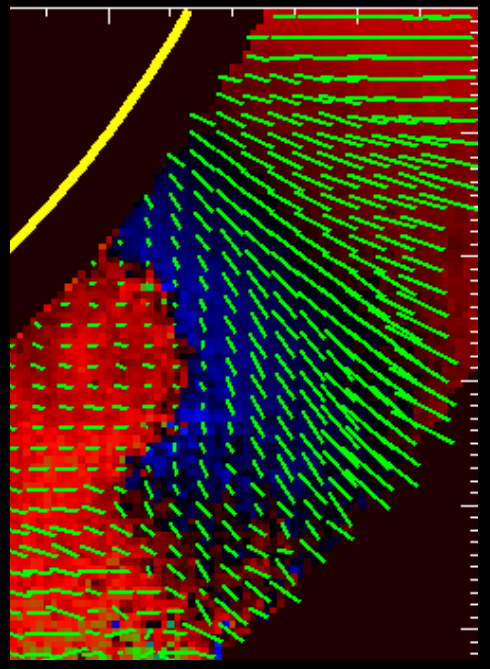

Non-radial expansion

Sarah Gibson, Urszula Bak-Steslicka, Giuliana de Toma, Laurel Rachmeler, Mei Zhang

Thanks to Yuhong Fan and Cooper Downs

Linear polarization in CoMP

Coronal Multichannel Polarimeter (CoMP)

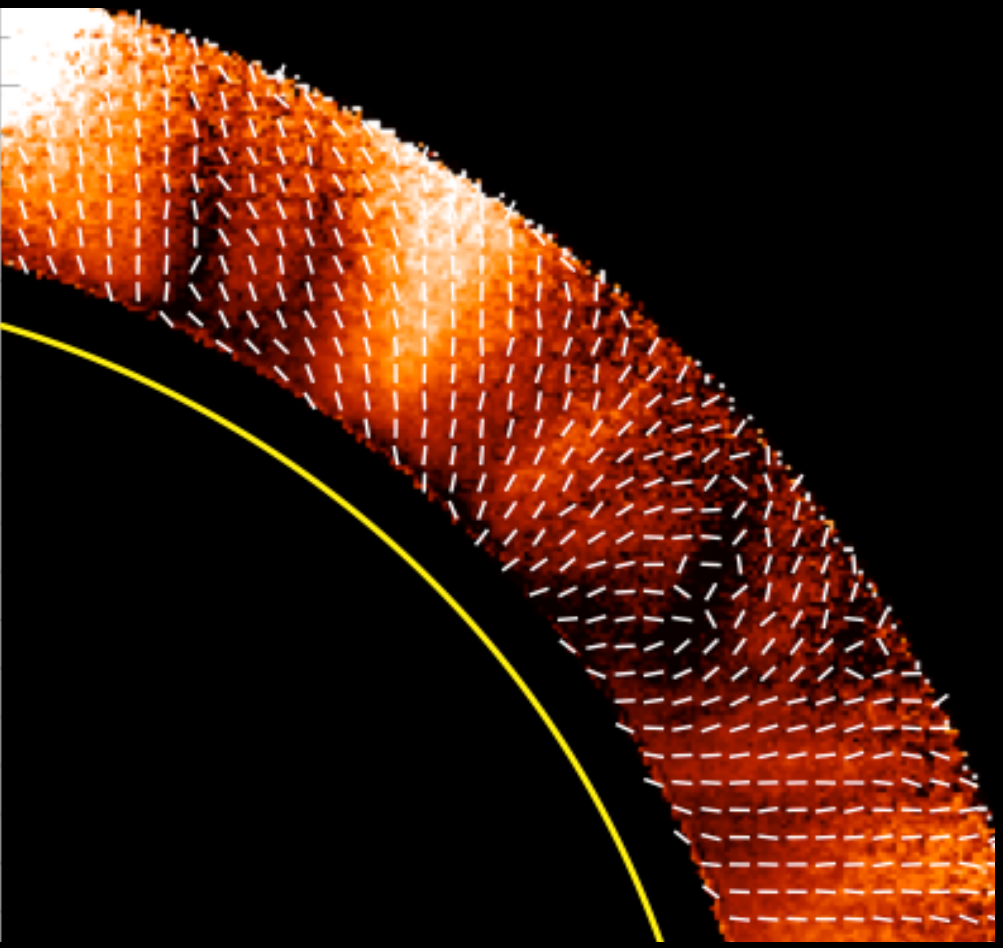

Linear polarization in CoMP

Coronal Multichannel Polarimeter (CoMP)

Daily (subject to weather), **full-sun** observations

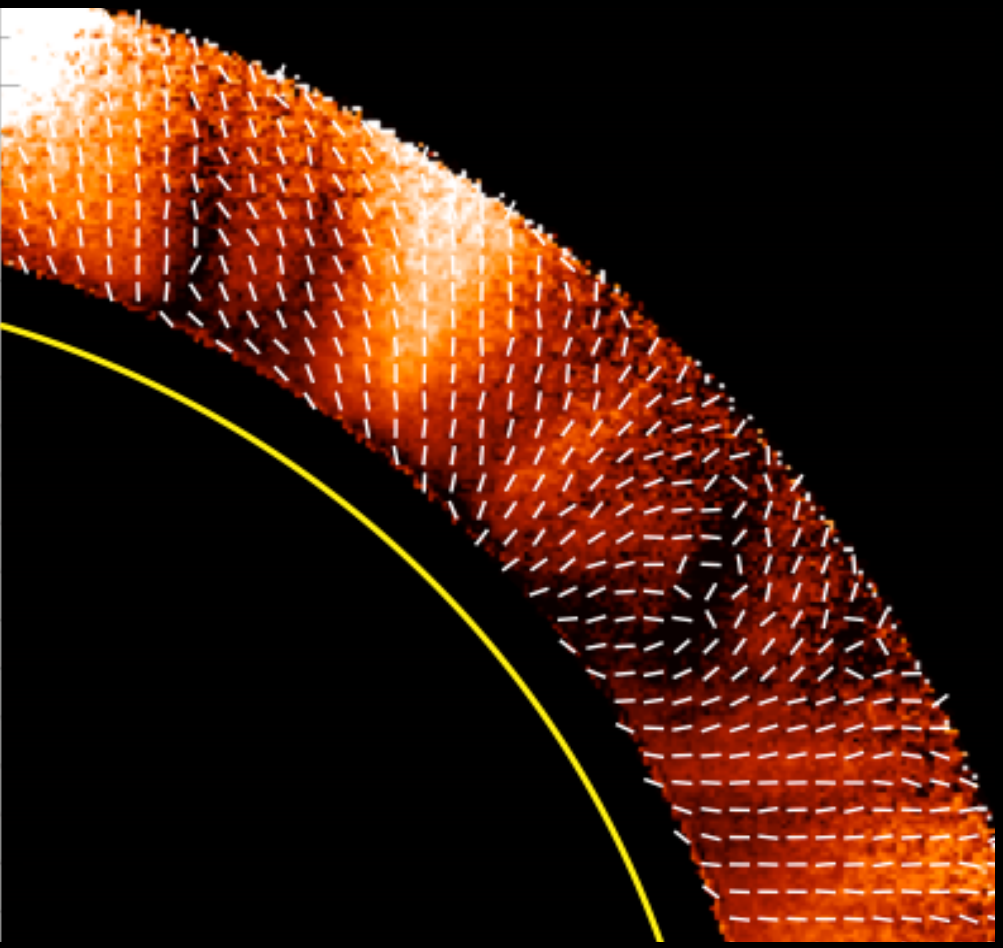

Linear polarization in CoMP

Coronal Multichannel Polarimeter (CoMP)

Daily (subject to weather), **full-sun** observations

Primary polarimetric observable:
L/I - fraction of linearly polarized light
($L = \sqrt{Q^2+U^2}$)

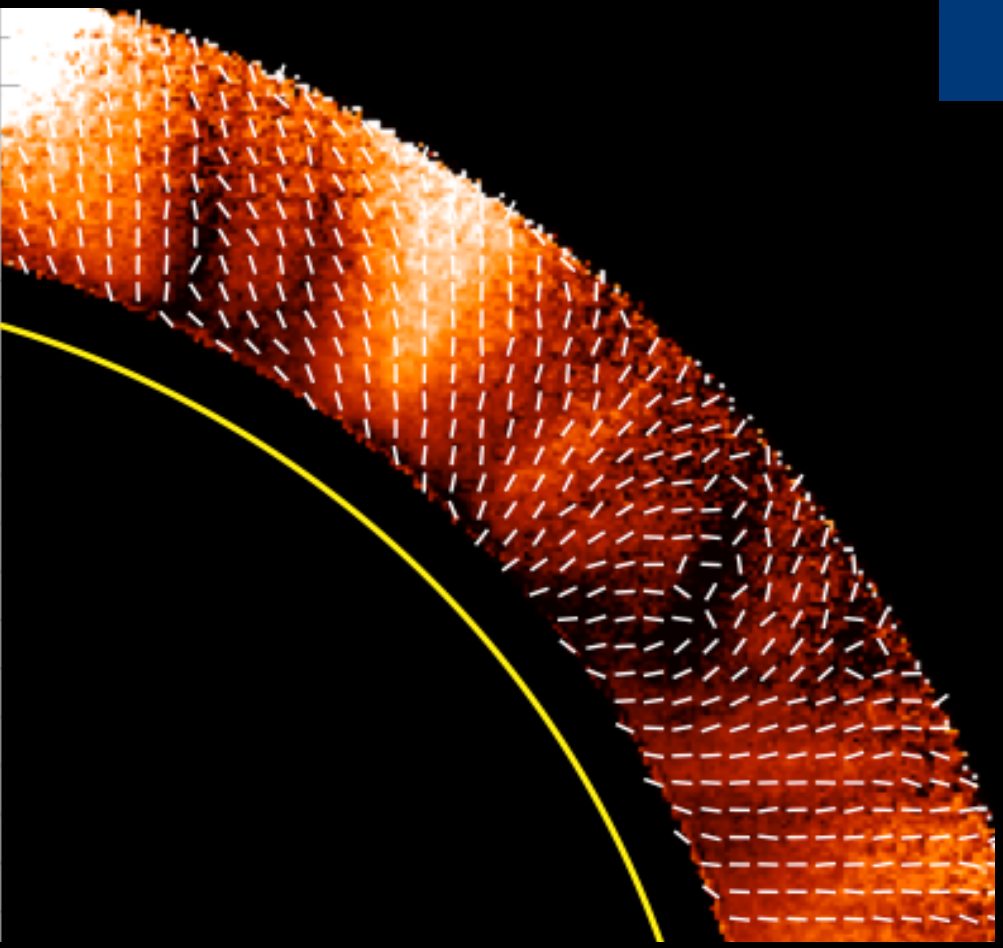

Linear polarization in CoMP

Coronal Multichannel Polarimeter (CoMP)

Daily (subject to weather), **full-sun** observations

Primary polarimetric observable:
L/I - fraction of linearly polarized light
($L = \sqrt{Q^2+U^2}$)

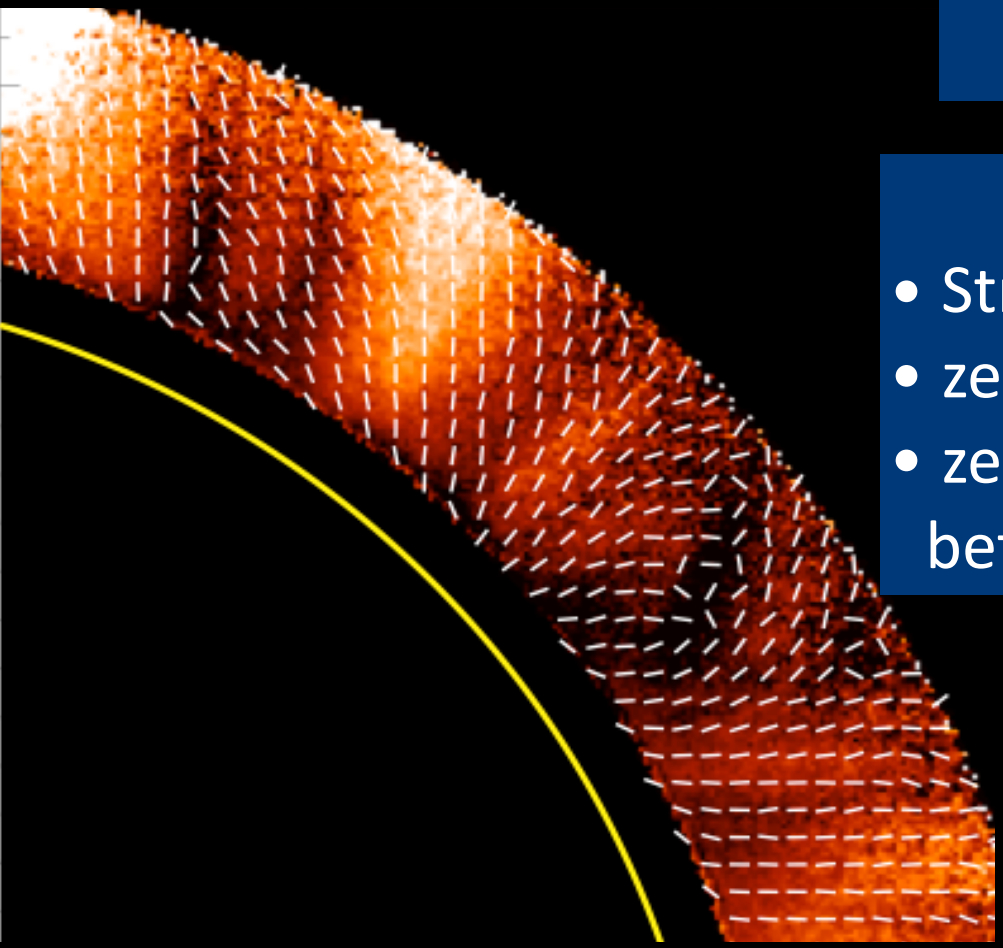

Hanle effect: depolarization

- Strong **L/I** signal: **B** in plane of sky (POS)
- zero: **B** along line of sight (LOS)
- zero: Van Vleck angle (measured between **B** and radial) = 54

Linear polarization in CoMP

Coronal Multichannel Polarimeter (CoMP)

Daily (subject to weather), **full-sun** observations

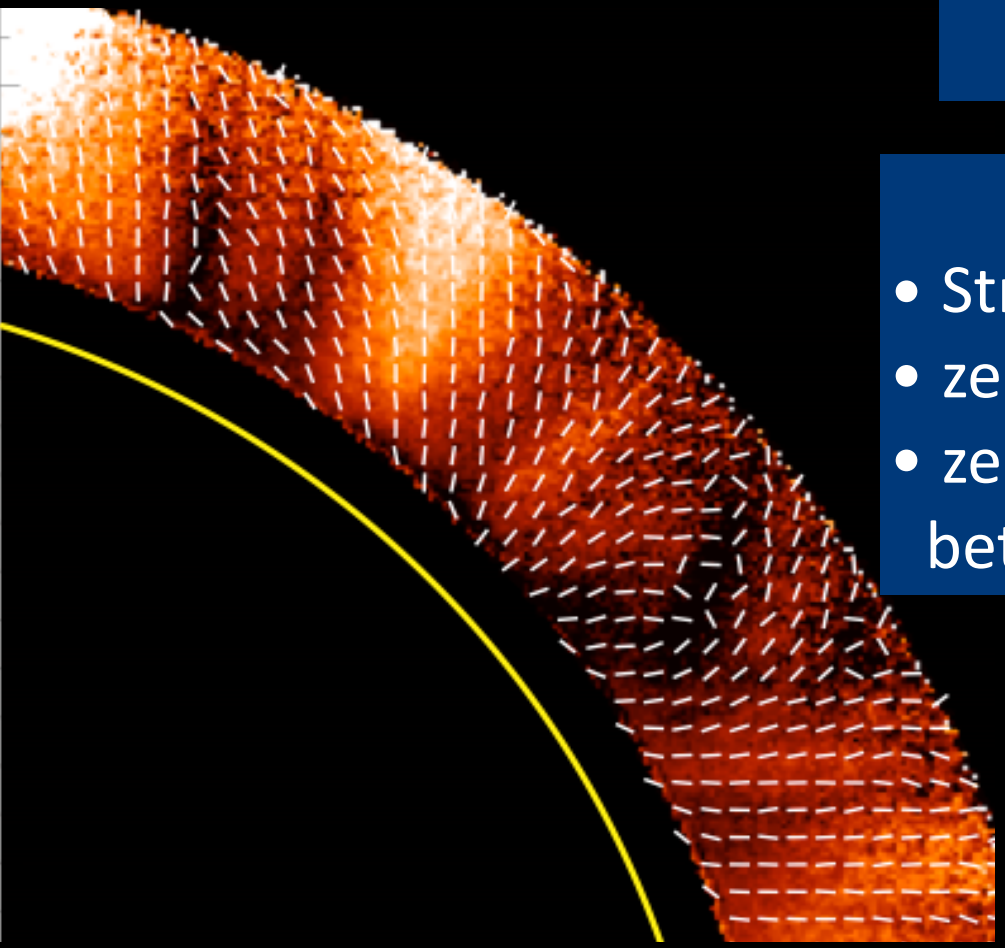

Primary polarimetric observable:
L/I - fraction of linearly polarized light
($L = \sqrt{Q^2+U^2}$)

Hanle effect: depolarization

- Strong **L/I** signal: **B** in plane of sky (POS)
- zero: **B** along line of sight (LOS)
- zero: Van Vleck angle (measured between **B** and radial) = 54

Direction of linear polarization = direction of POS vector (but rotates 90 degrees at V. V. angle!)

Linear polarization in CoMP

Coronal Multichannel Polarimeter (CoMP)

Daily (subject to weather), **full-sun** observations

Line of Sight Integrated

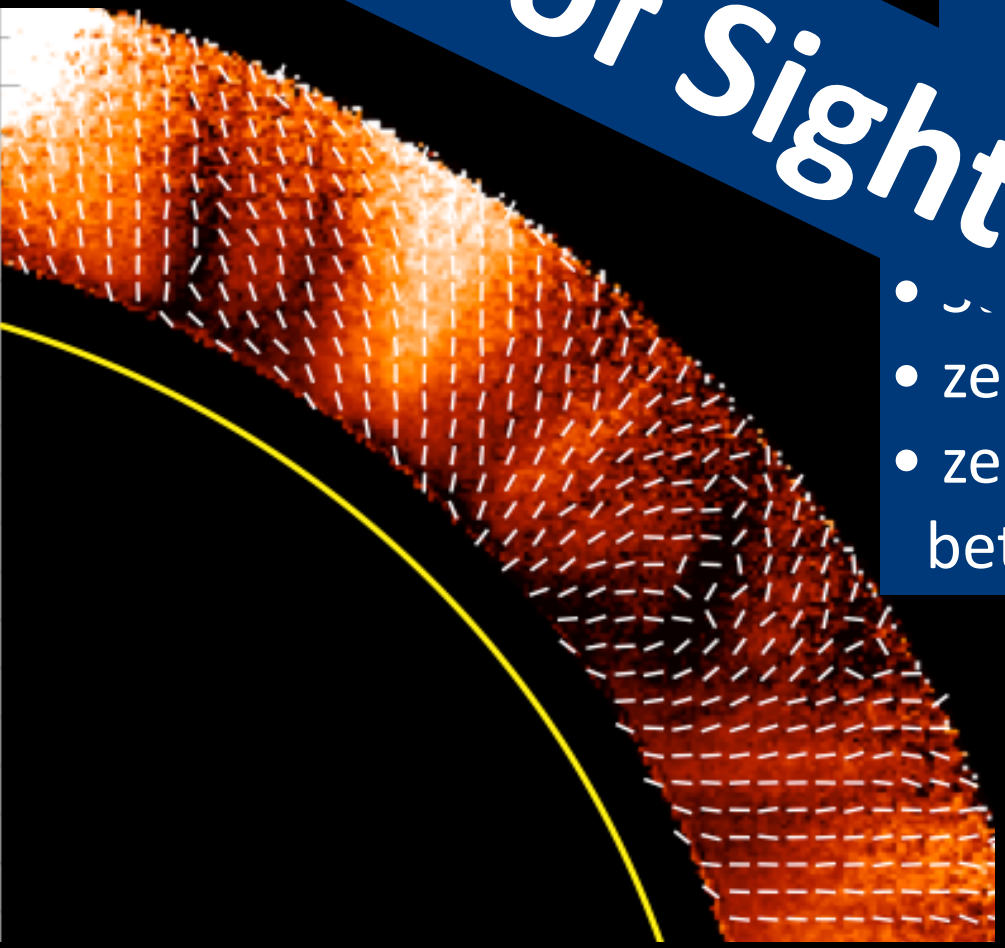

Primary polarimetric observable:
L/I - fraction of linearly polarized light
($L = \sqrt{Q^2+U^2}$)

ffect: depolarization

- in plane of sky (POS)
- zero: B (LOS)
- zero: Van Vle ed between **B** and radia

Direction of linear polarization = direction of POS vector (but rotates 90 degrees at V. V. angle!)

Linear polarization in CoMP

Coronal Multichannel Polarimeter (CoMP)

Daily (subject to weather), **full-sun** observations

Line of Sight Integrated

Primary polarimetric observable:
L/I - fraction of linearly polarized light
($L = \sqrt{Q^2+U^2}$)

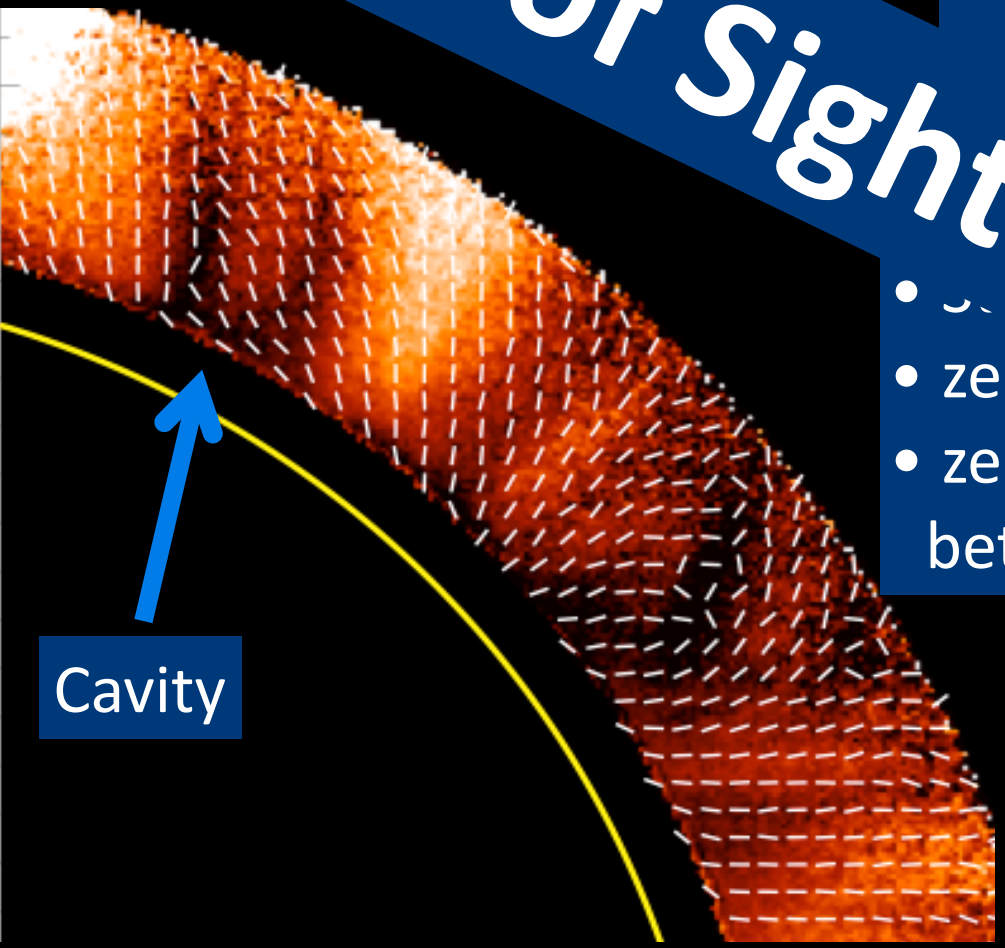

ffect: depolarization

- in plane of sky (POS)
- zero: B (LOS)
- zero: Van Vle ed between **B** and radia

Direction of linear polarization = direction of POS vector (but rotates 90 degrees at V. V. angle!)

Lagomorphs in CoMP linear polarization

EUV coronal cavities = CoMP lagomorphs

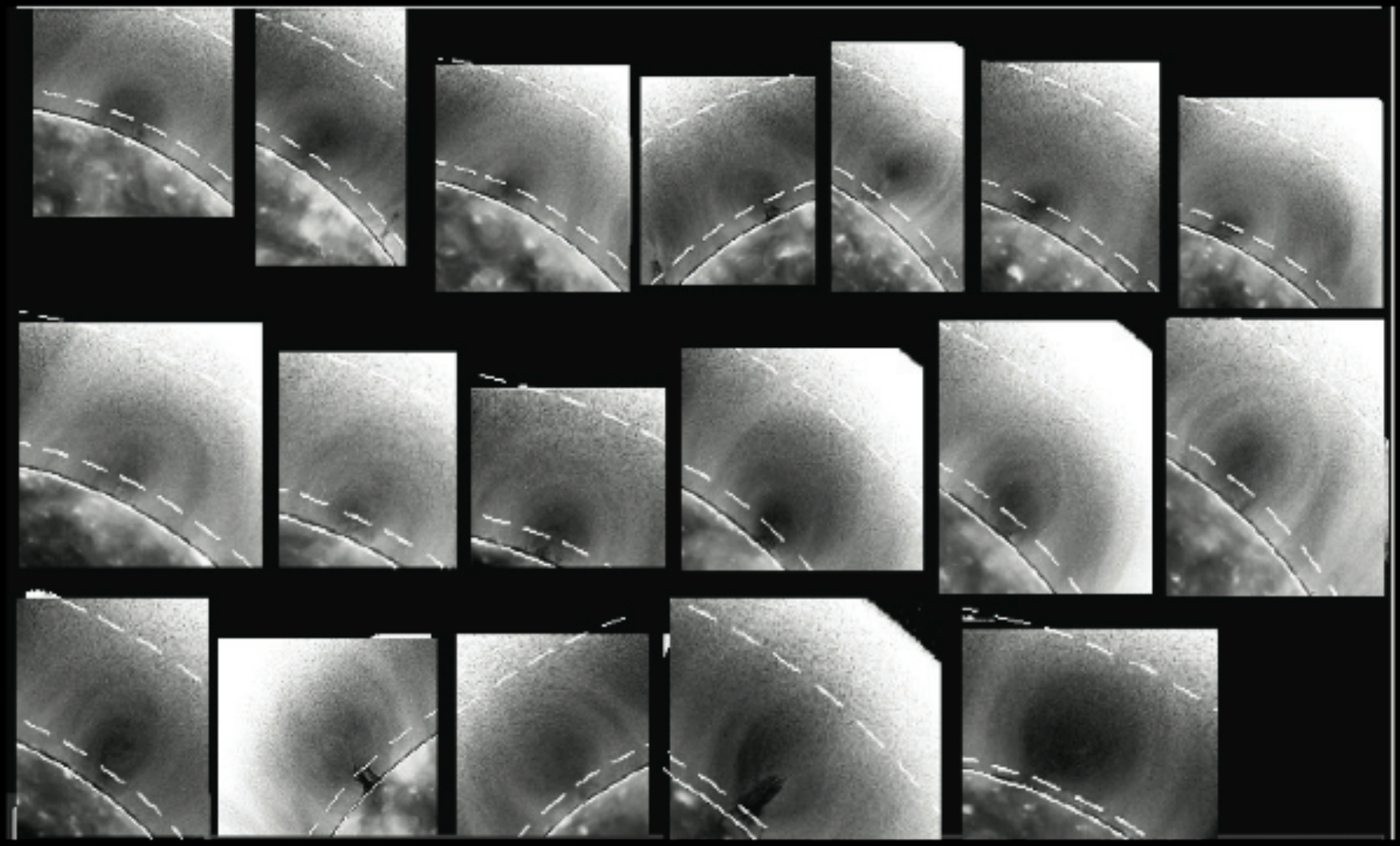

Gibson, 2014

Lagomorphs in CoMP linear polarization

EUV coronal cavities = CoMP lagomorphs

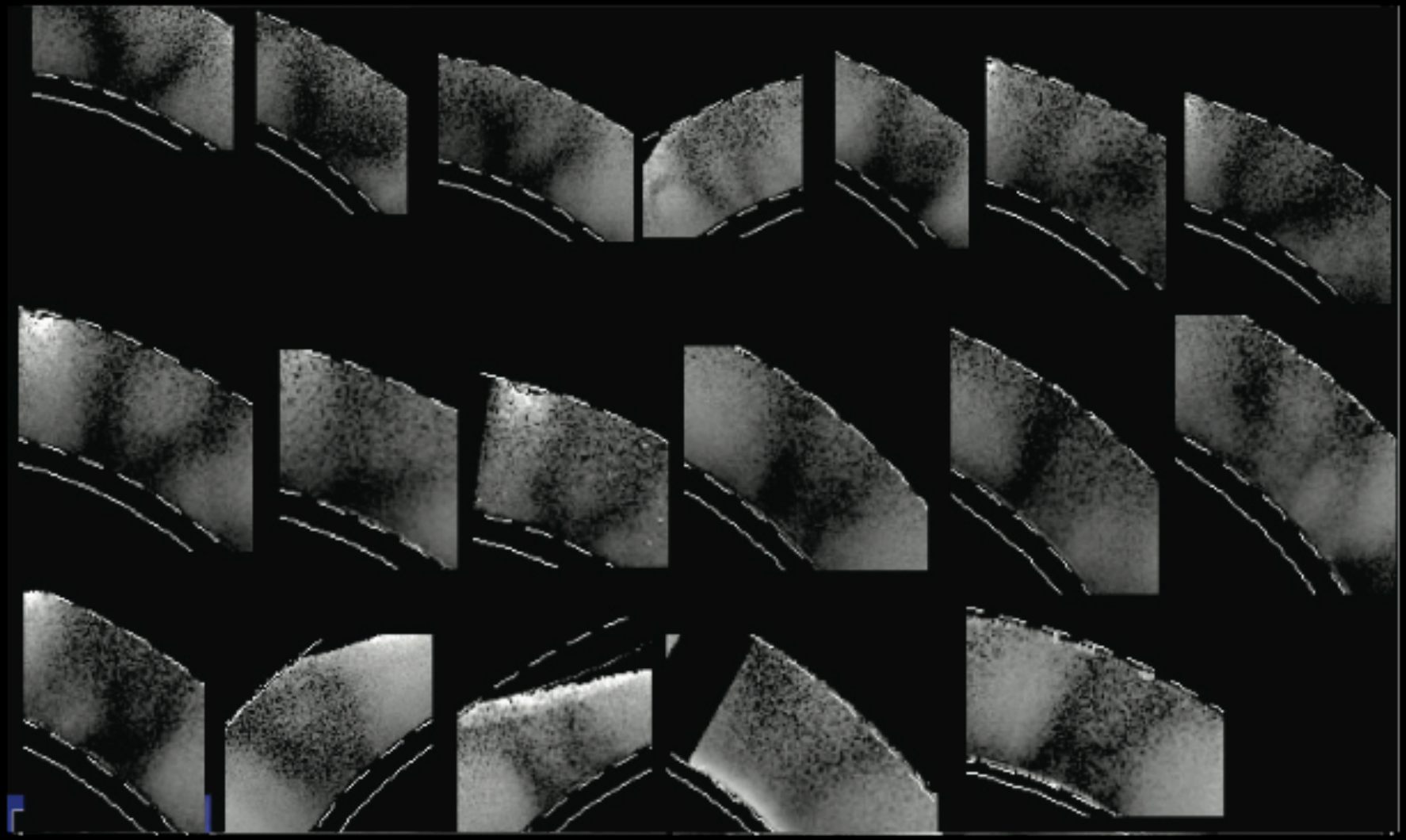

Gibson, 2014

Lagomorphs, cavities and flux ropes

DATA

MODEL

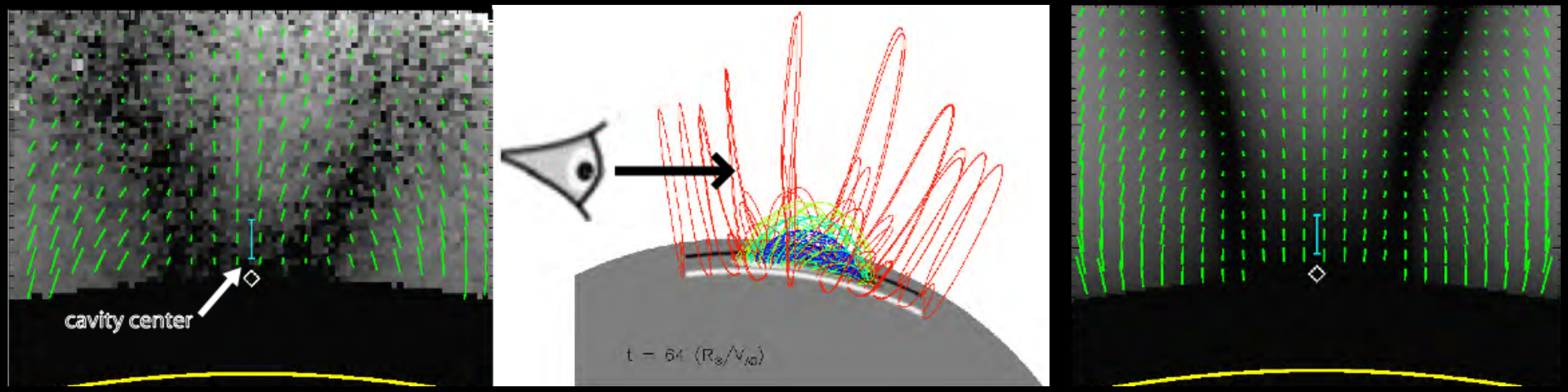

Diagnostic of magnetic flux rope

Model B (POS)

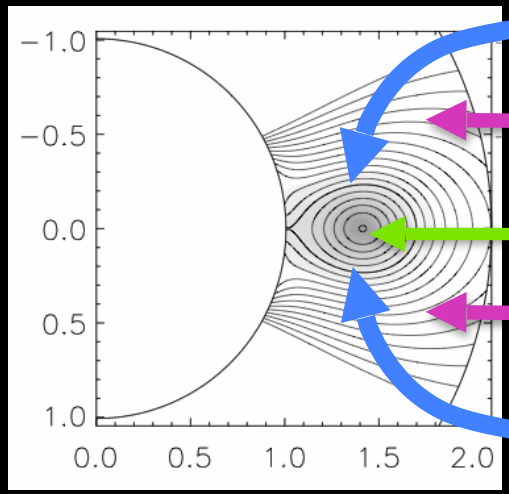

Van Vleck inversion in flux rope

Van Vleck inversion in arcade

Flux rope axis

Model L/I (POS)

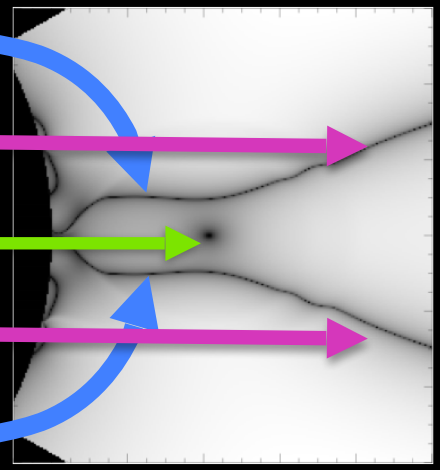

Bak-Steslicka et al., 2013

Lagomorphs, cavities and flux ropes

Axial (LOS-aligned) field at cavity center — above prominence

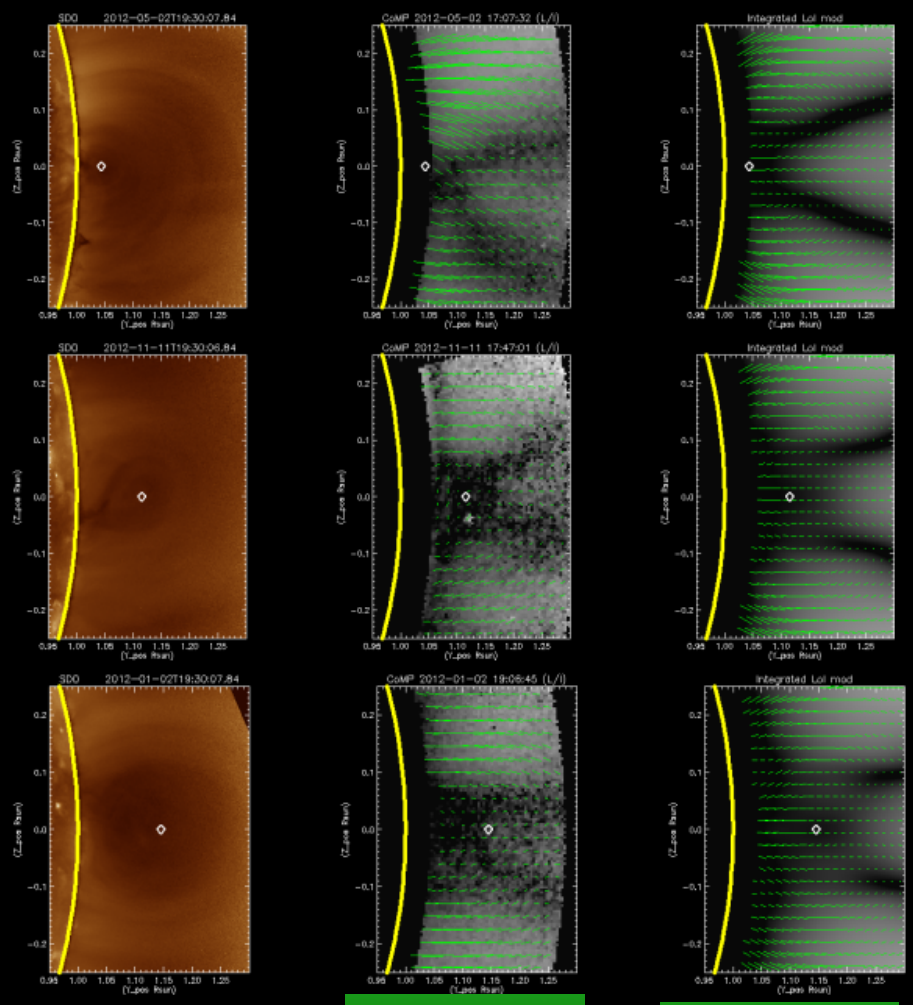

EUV cavity

CoMP lagomorph

Forward-modeled flux ropes

Bak-Steslicka et al., 2014; 2016, Gibson, 2015; Fan, 2012

Lagomorphs, cavities and flux ropes

Axial (LOS-aligned) field at cavity center — above prominence

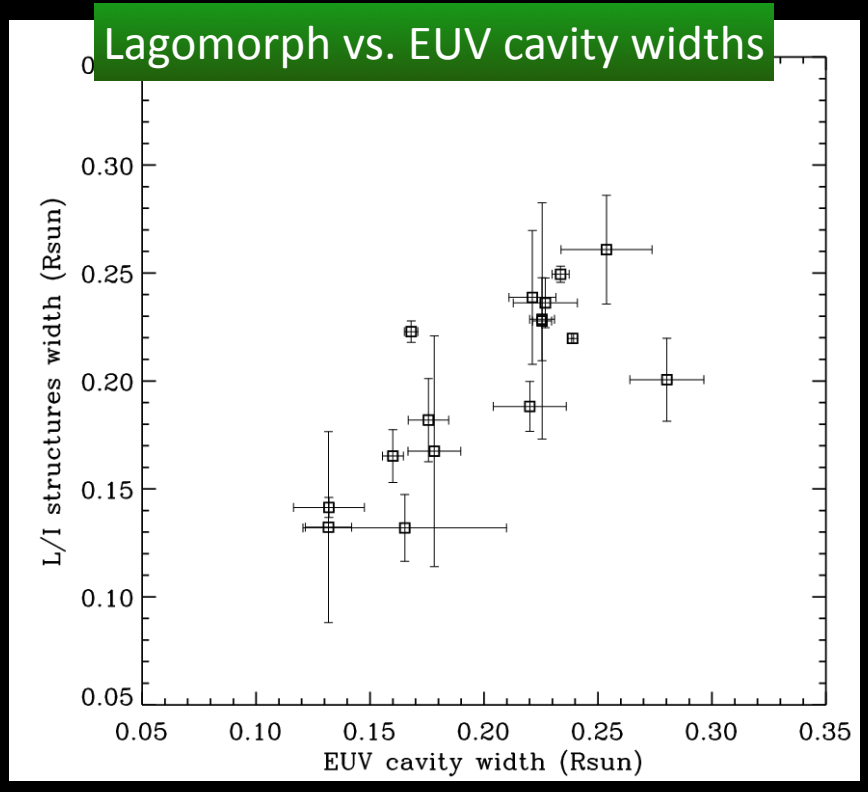

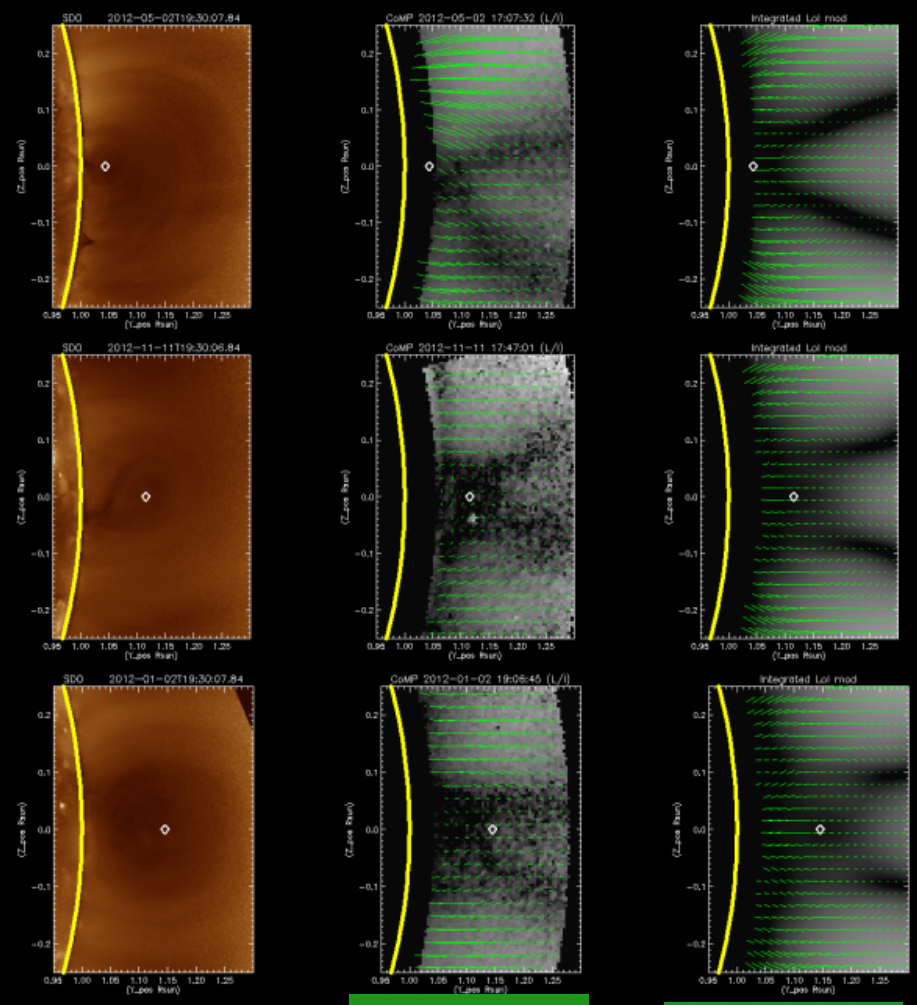

EUV cavity

CoMP lagomorph

Forward-modeled flux ropes

Bak-Steslicka et al., 2014; 2016, Gibson, 2015; Fan, 2012

Lagomorphs, cavities and flux ropes

Axial (LOS-aligned) field at cavity center — above prominence

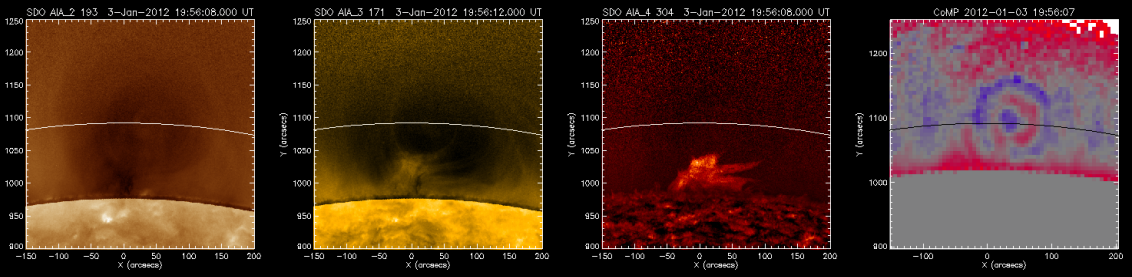

EUV cavity

Prominence

CoMP Doppler Vlos

Lagomorph vs. EUV cavity widths

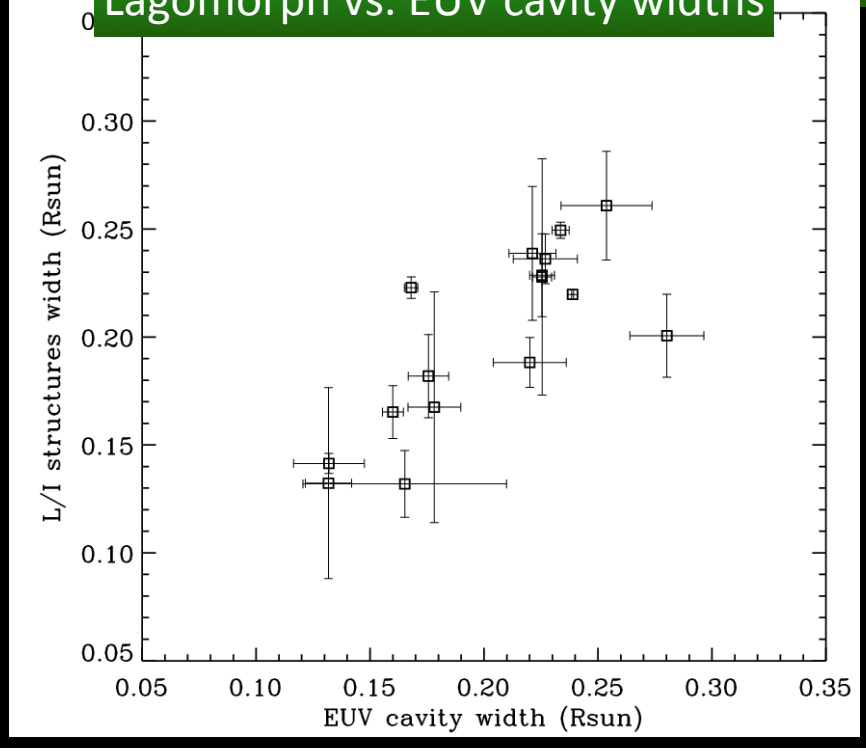

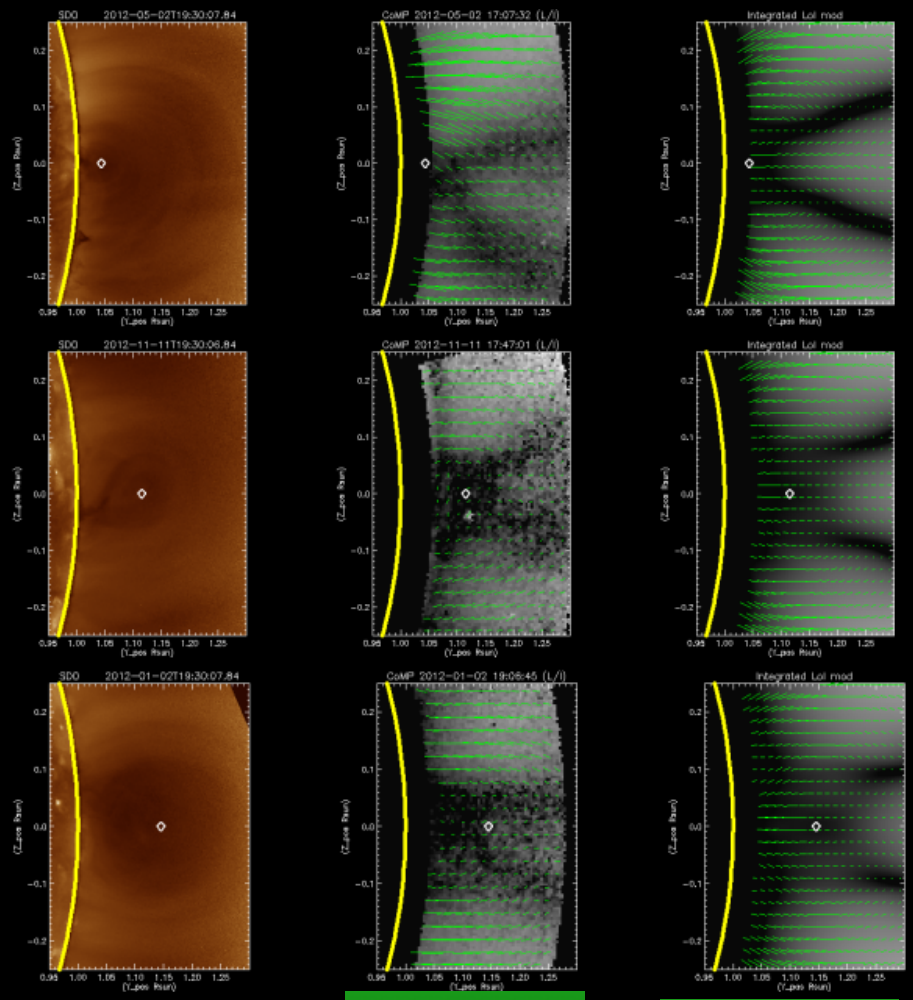

EUV cavity

CoMP lagomorph

Forward-modeled flux ropes

Bak-Steslicka et al., 2014; 2016, Gibson, 2015; Fan, 2012

Lagomorphs, cavities and flux ropes

Axial (LOS-aligned) field at cavity center — above prominence

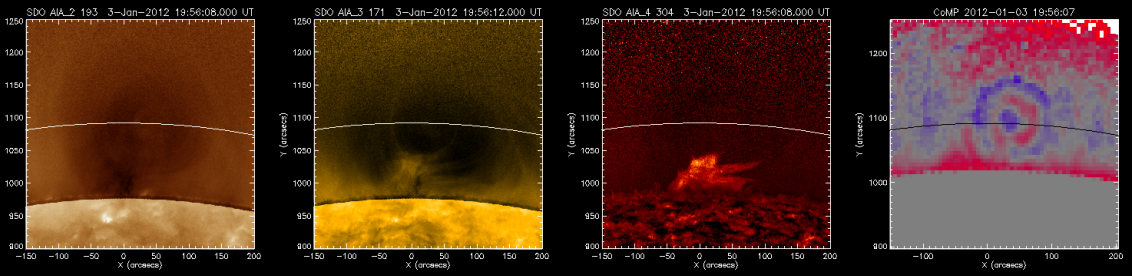

EUV cavity

Prominence

CoMP Doppler Vlos

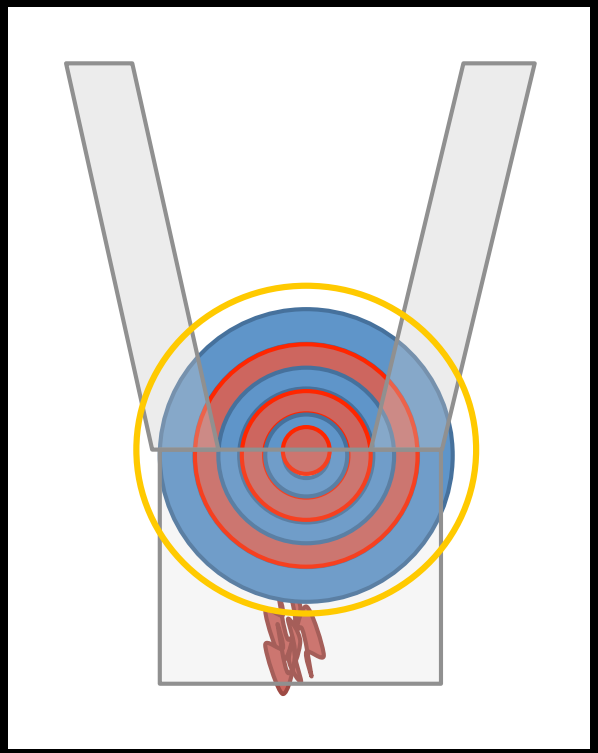

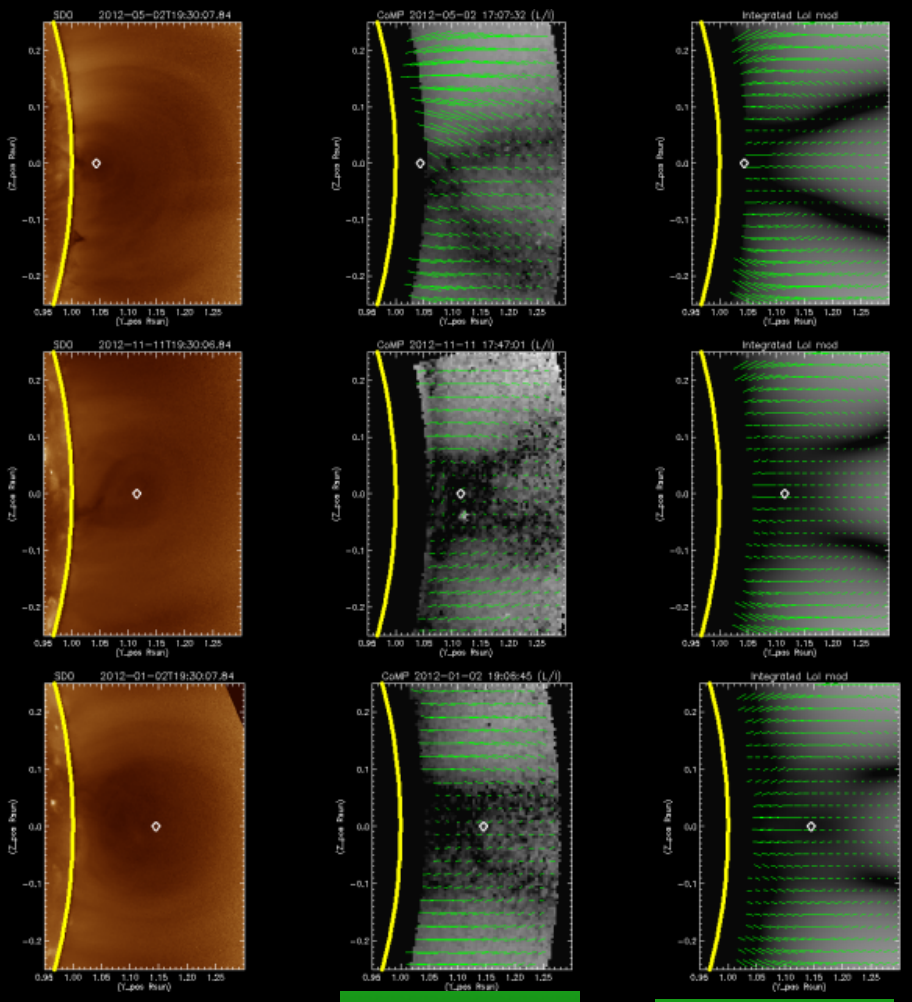

EUV cavity

CoMP lagomorph

Forward-modeled flux ropes

Bak-Steslicka et al., 2014; 2016, Gibson, 2015; Fan, 2012

Lagomorphs, cavities and flux ropes

Axial (LOS-aligned) field at cavity center — above prominence

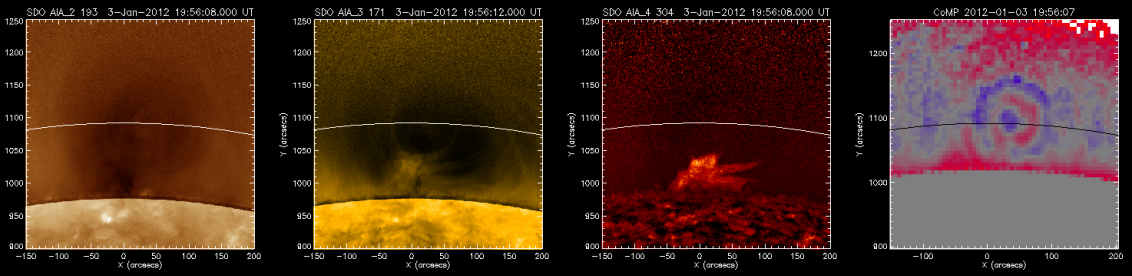

EUV cavity

Prominence

CoMP Doppler Vlos

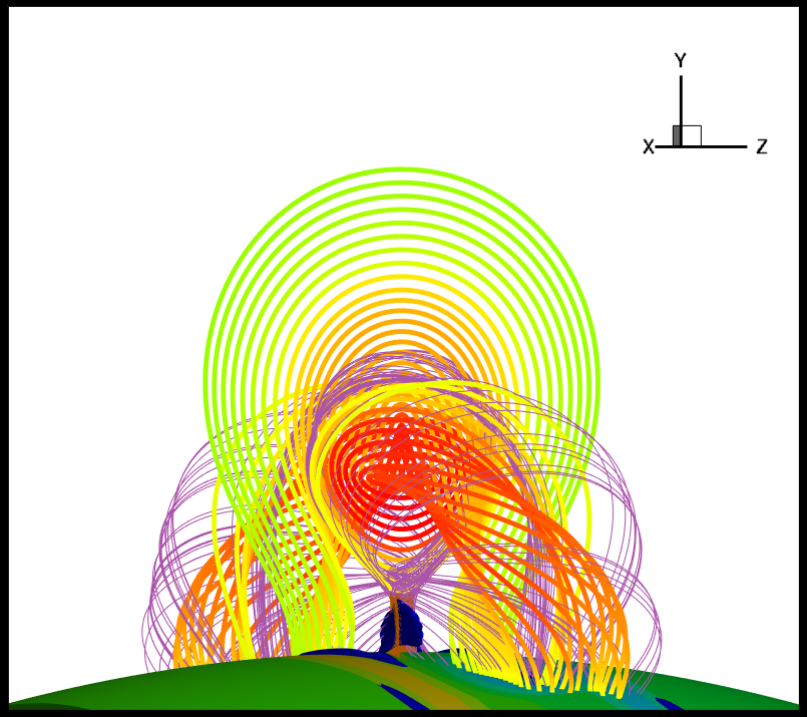

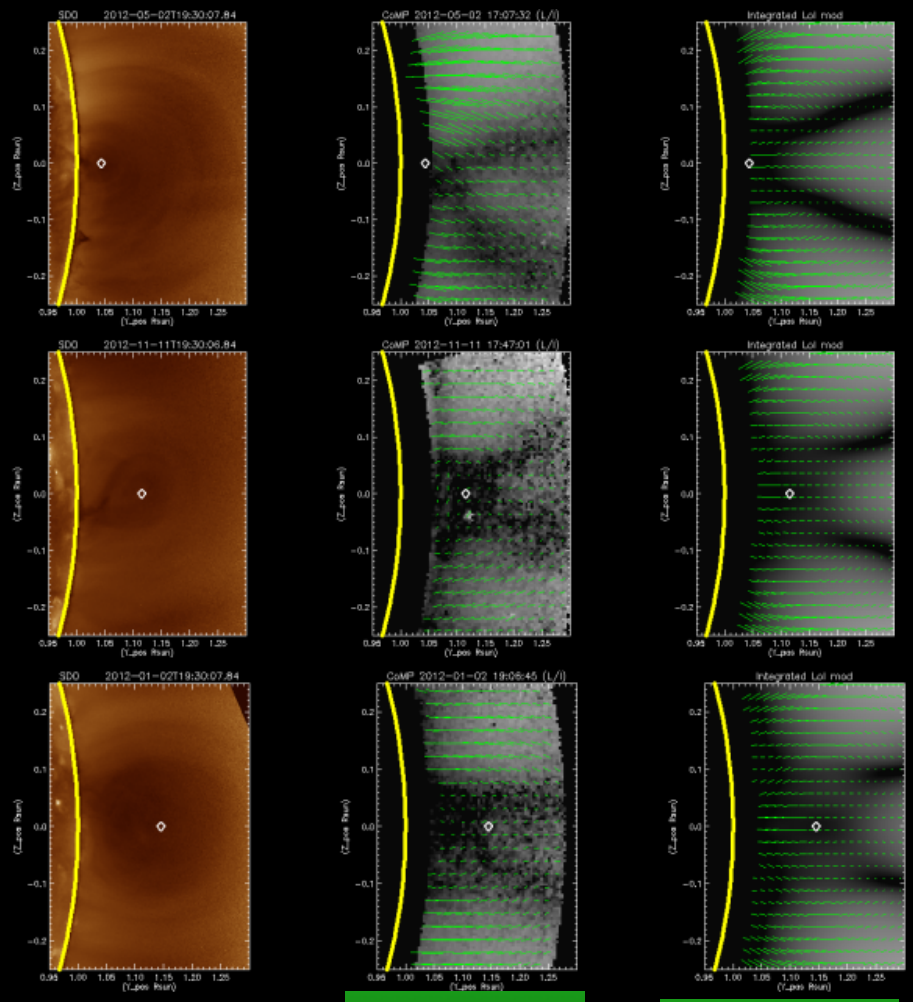

EUV cavity

CoMP lagomorph

Forward-modeled flux ropes

Bak-Steslicka et al., 2014; 2016, Gibson, 2015; Fan, 2012

Cavities, flux ropes and torus instability

Near-erupting cavity: index = ~1.4 at cavity center

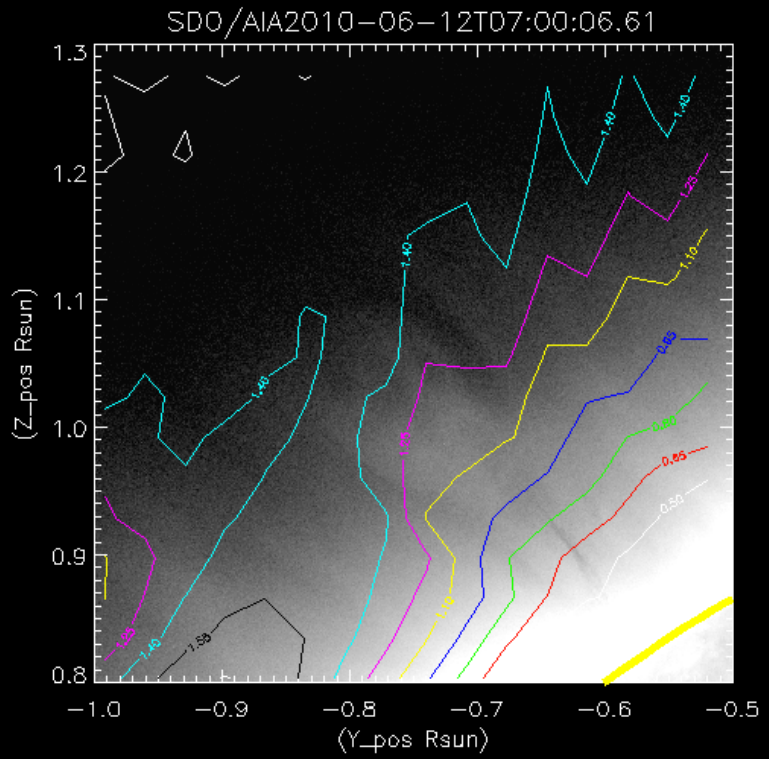

Stable cavity: index = ~0.8 at cavity center

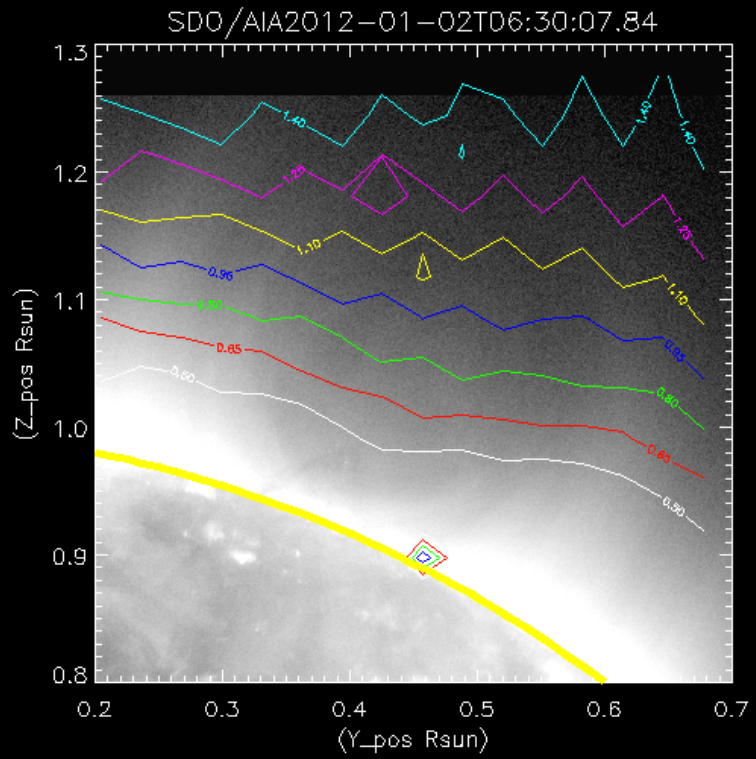

Cavities, flux ropes and torus instability

Near-erupting cavity: index = ~1.4 at cavity center

Stable cavity: index = ~0.8 at cavity center

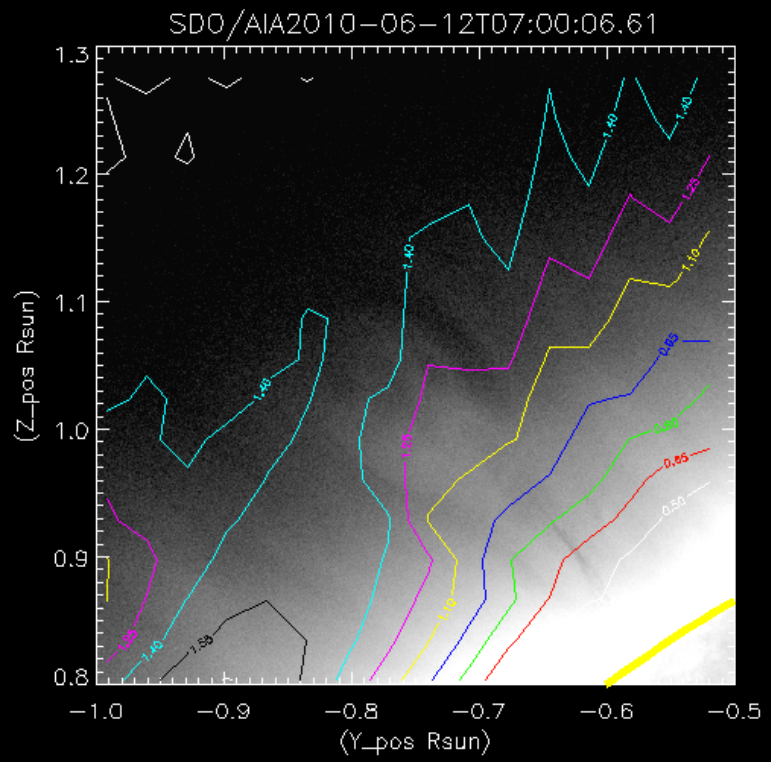

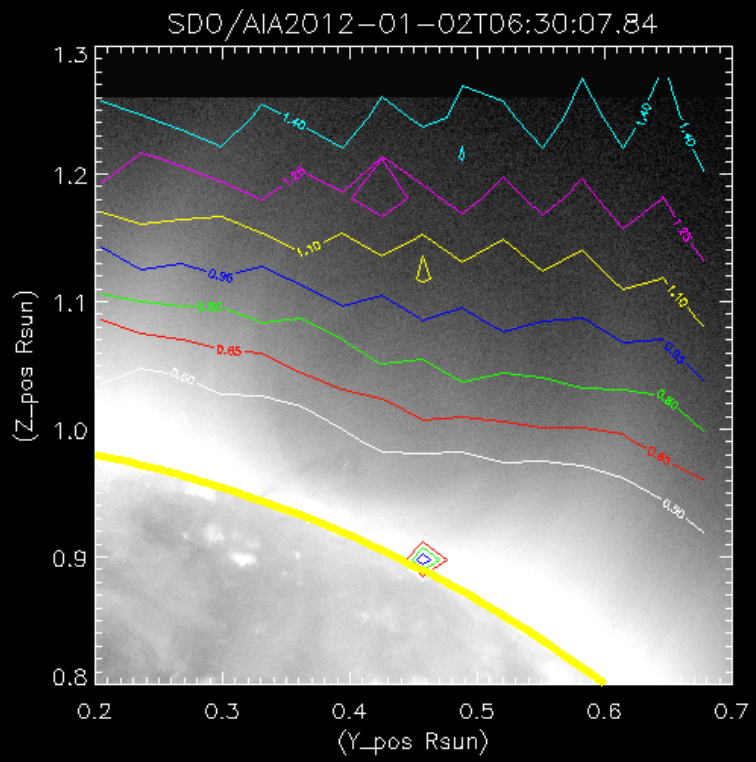

Light-blue contour = index=1.4

Cavities, flux ropes and torus instability

de Toma — poster

Nonerupting “simple” cavities tend to have lower instability index than erupting cavities

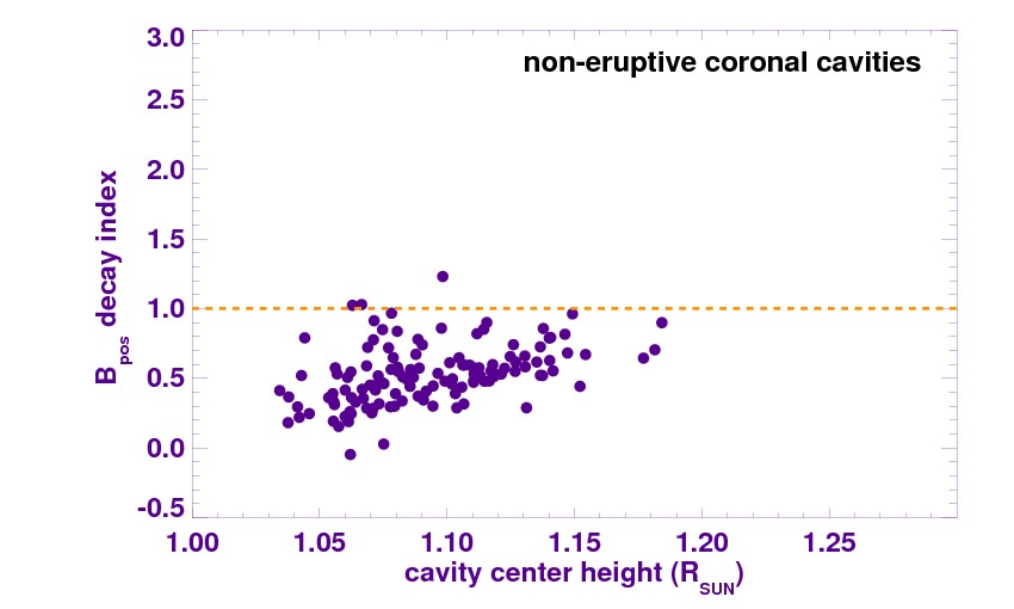

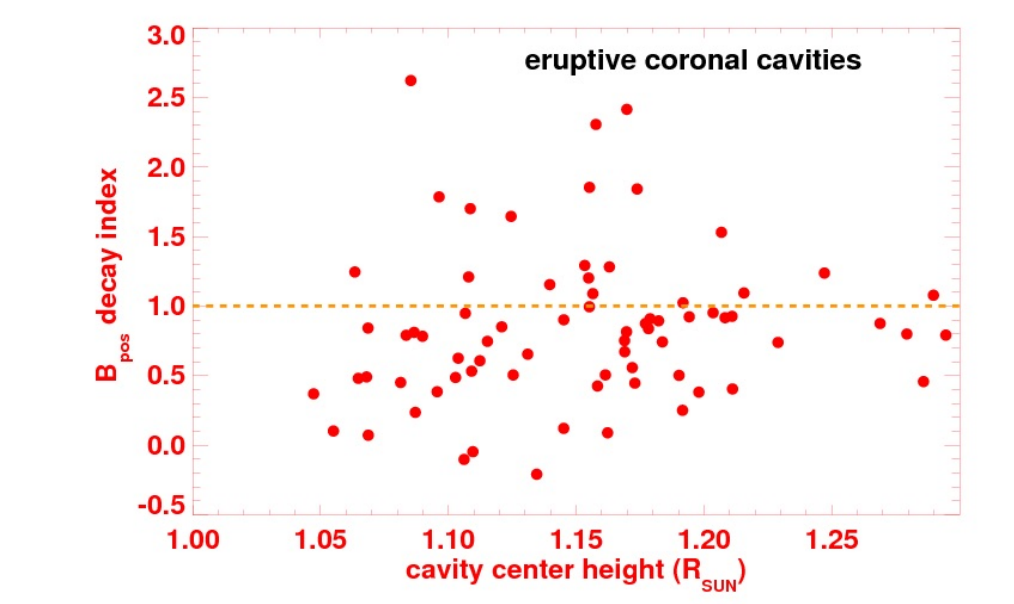

Cavities, flux ropes and torus instability

de Toma — poster

Nonerupting “simple” cavities tend to have lower instability index than erupting cavities

HOWEVER!!!!

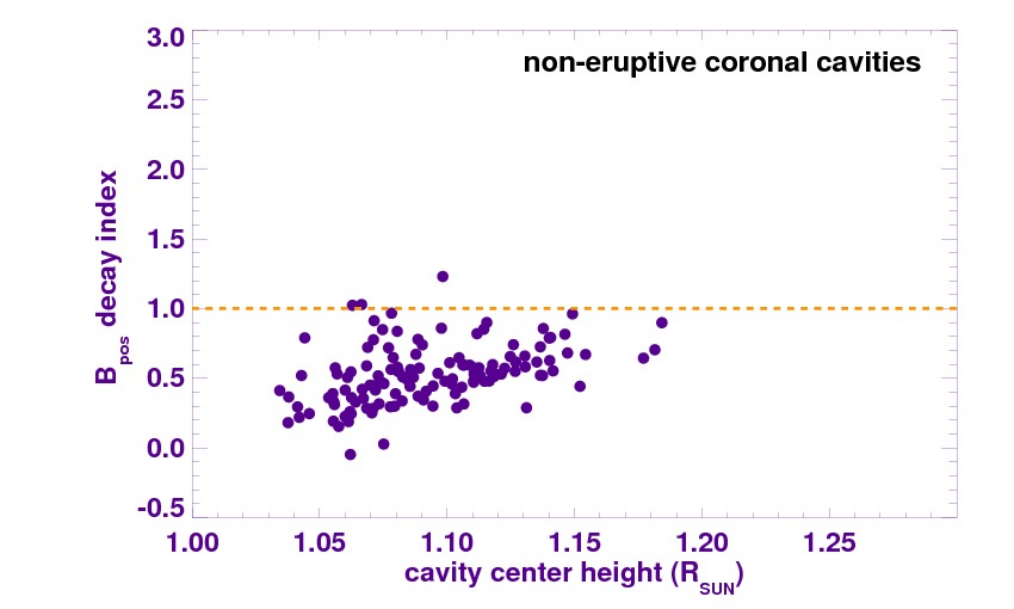

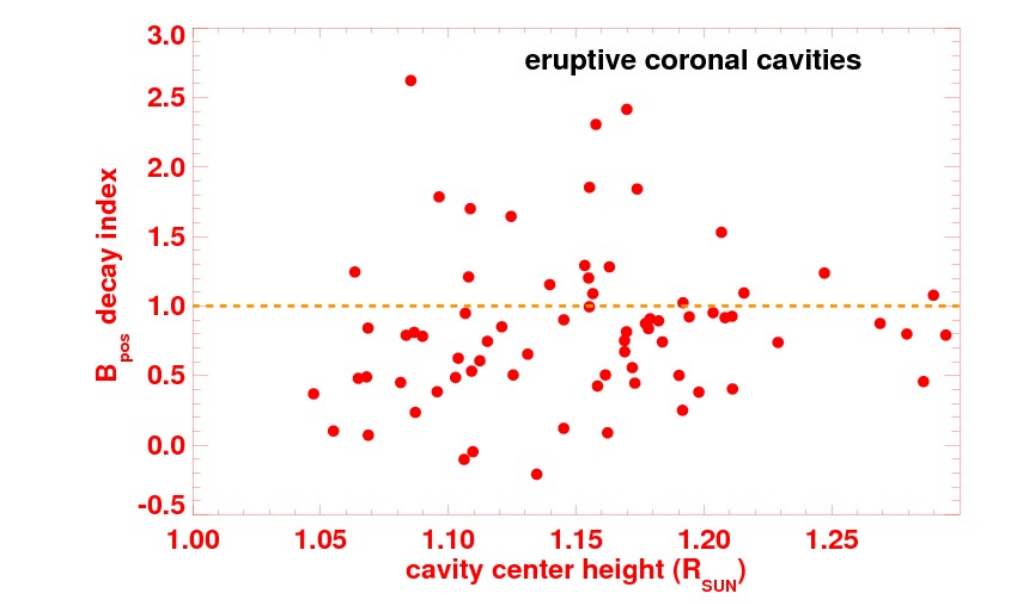

Cavities, flux ropes and torus instability

de Toma — poster

Nonerupting “simple” cavities tend to have lower instability index than erupting cavities

HOWEVER!!!!

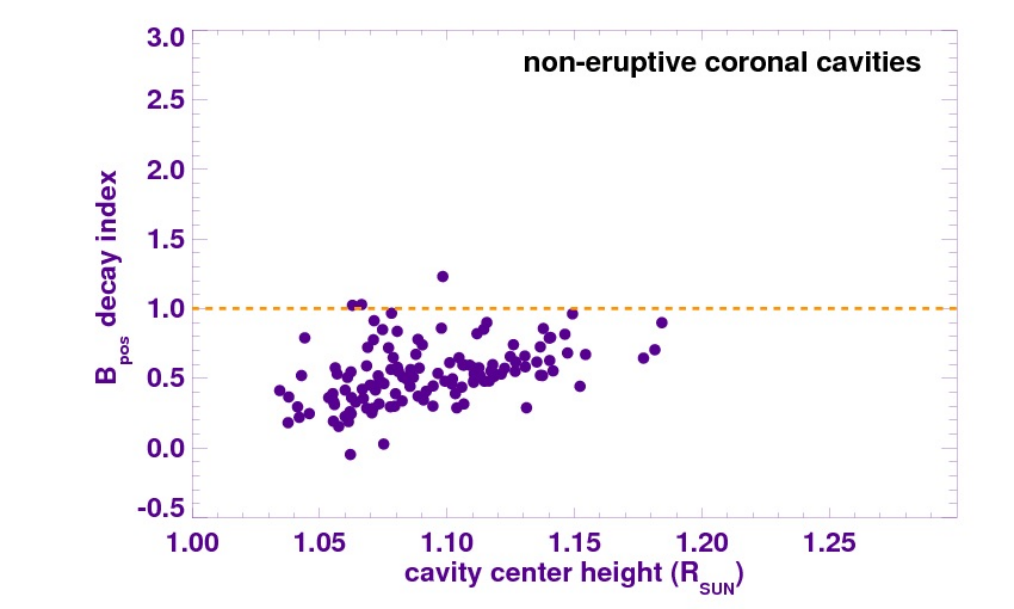

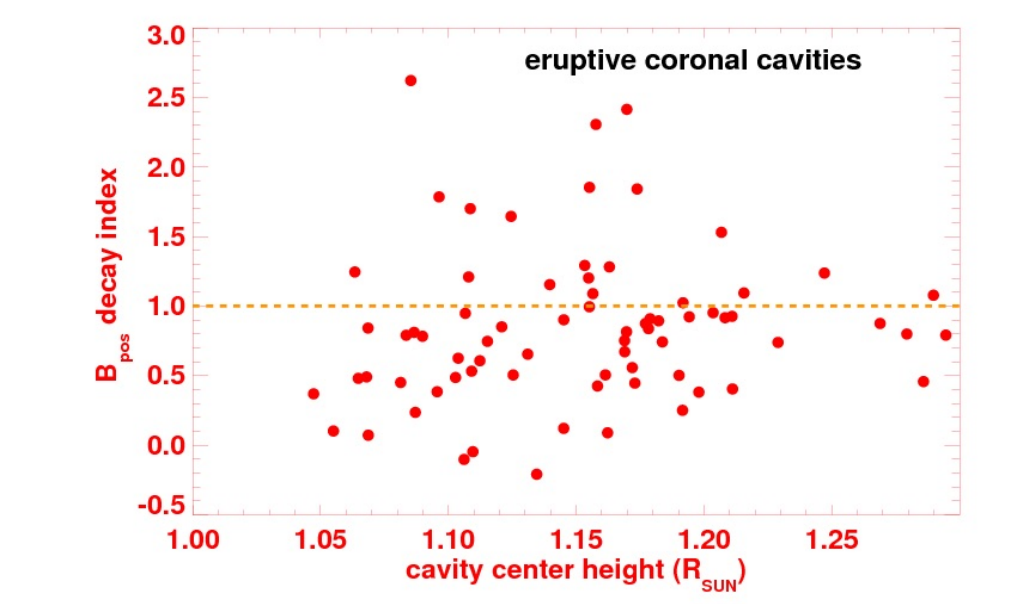

Trend does not hold for “complex” cavities

Cavities, flux ropes and torus instability

de Toma — poster

Nonerupting “simple” cavities tend to have lower instability index than erupting cavities

HOWEVER!!!!

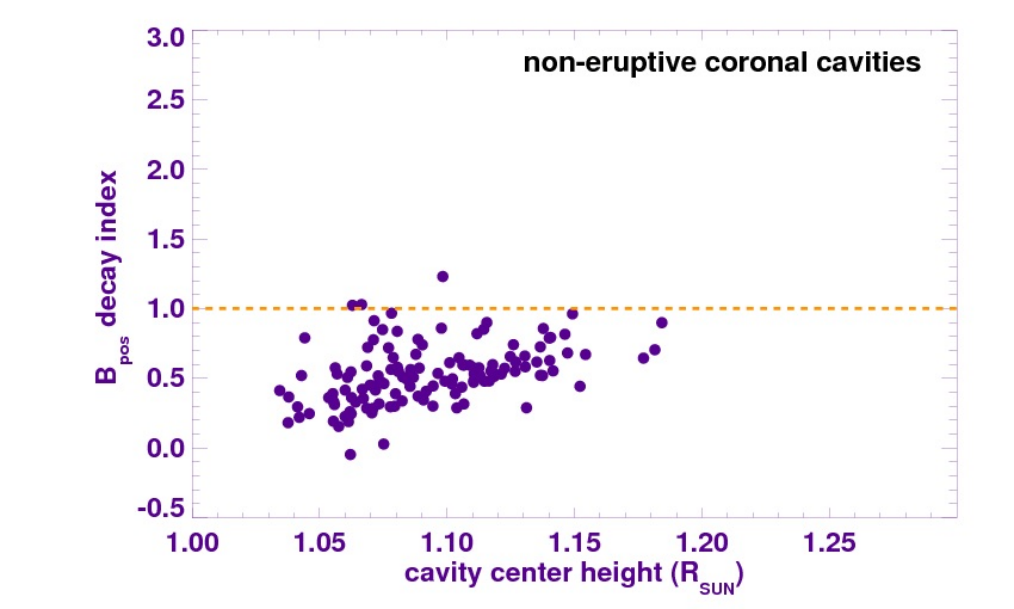

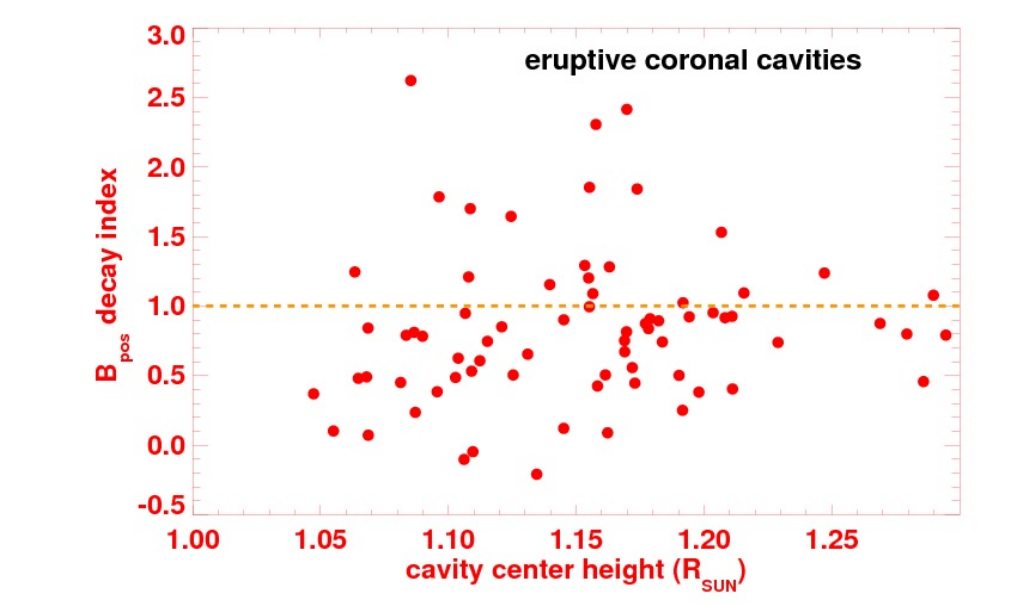

Trend does not hold for “complex” cavities

PSEUDOSTREAMERS

Cavities, flux ropes and torus instability

de Toma — poster

Nonerupting “simple” cavities tend to have lower instability index than erupting cavities

HOWEVER!!!!

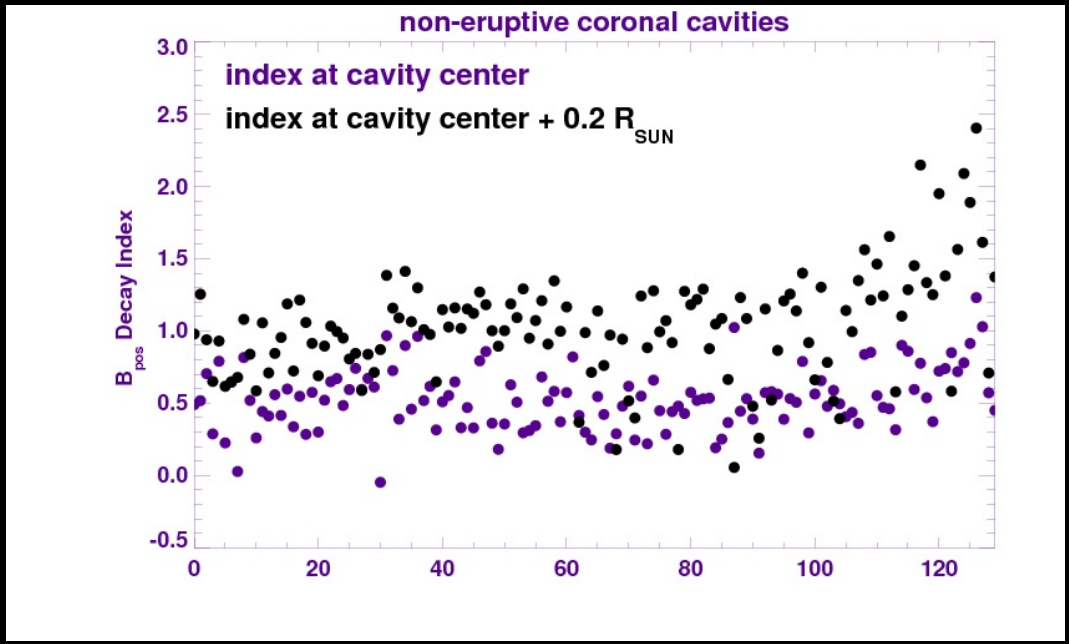

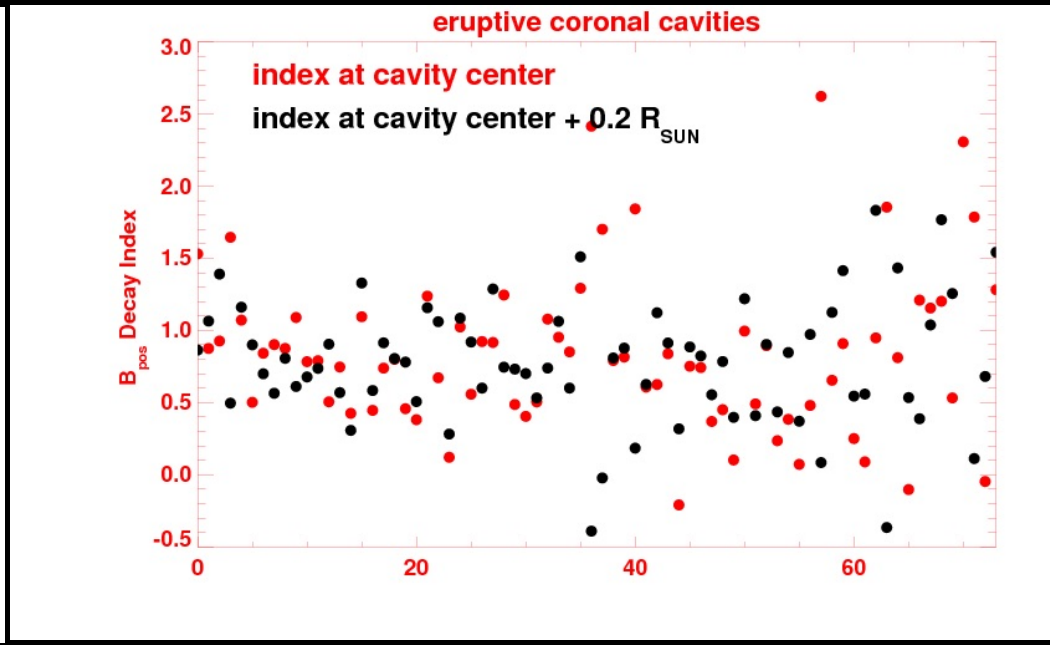

Trend does not hold for “complex” cavities

Cavities, flux ropes and torus instability

de Toma — poster

Nonerupting “simple” cavities tend to have lower instability index than erupting cavities

HOWEVER!!!!

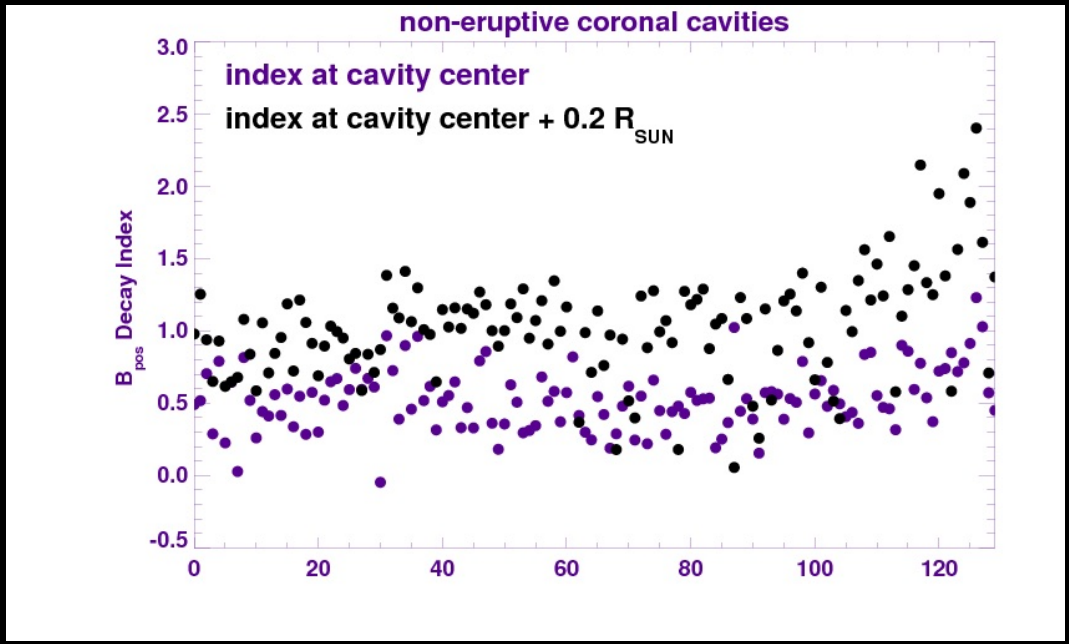

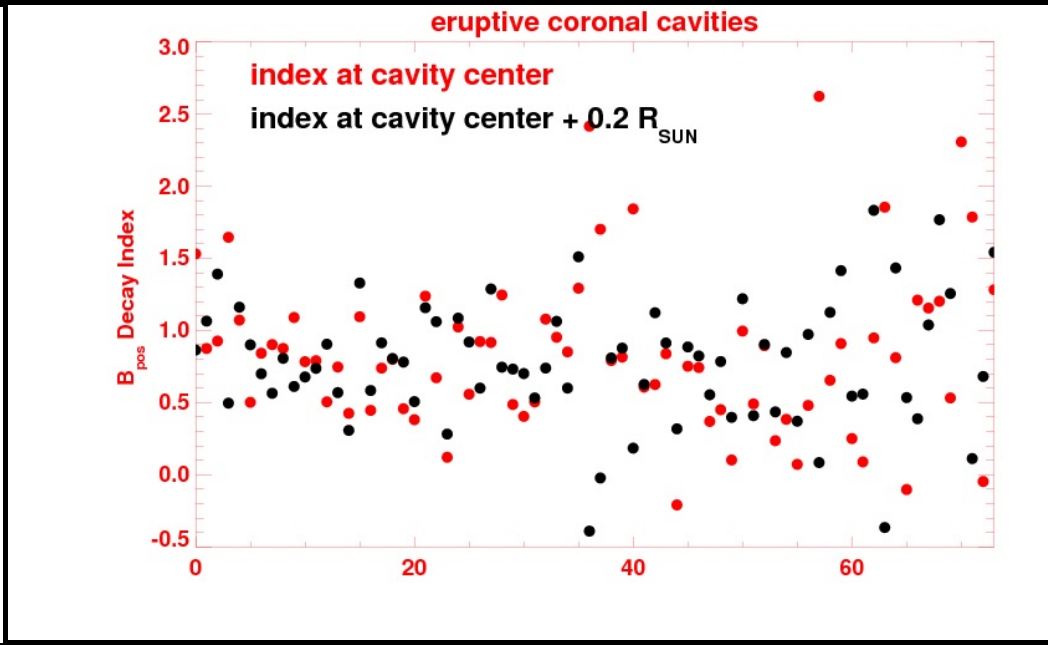

Trend does not hold for “complex” cavities

PSEUDOSTREAMERS

Pseudostreamers in CoMP linear polarization

Expected topology

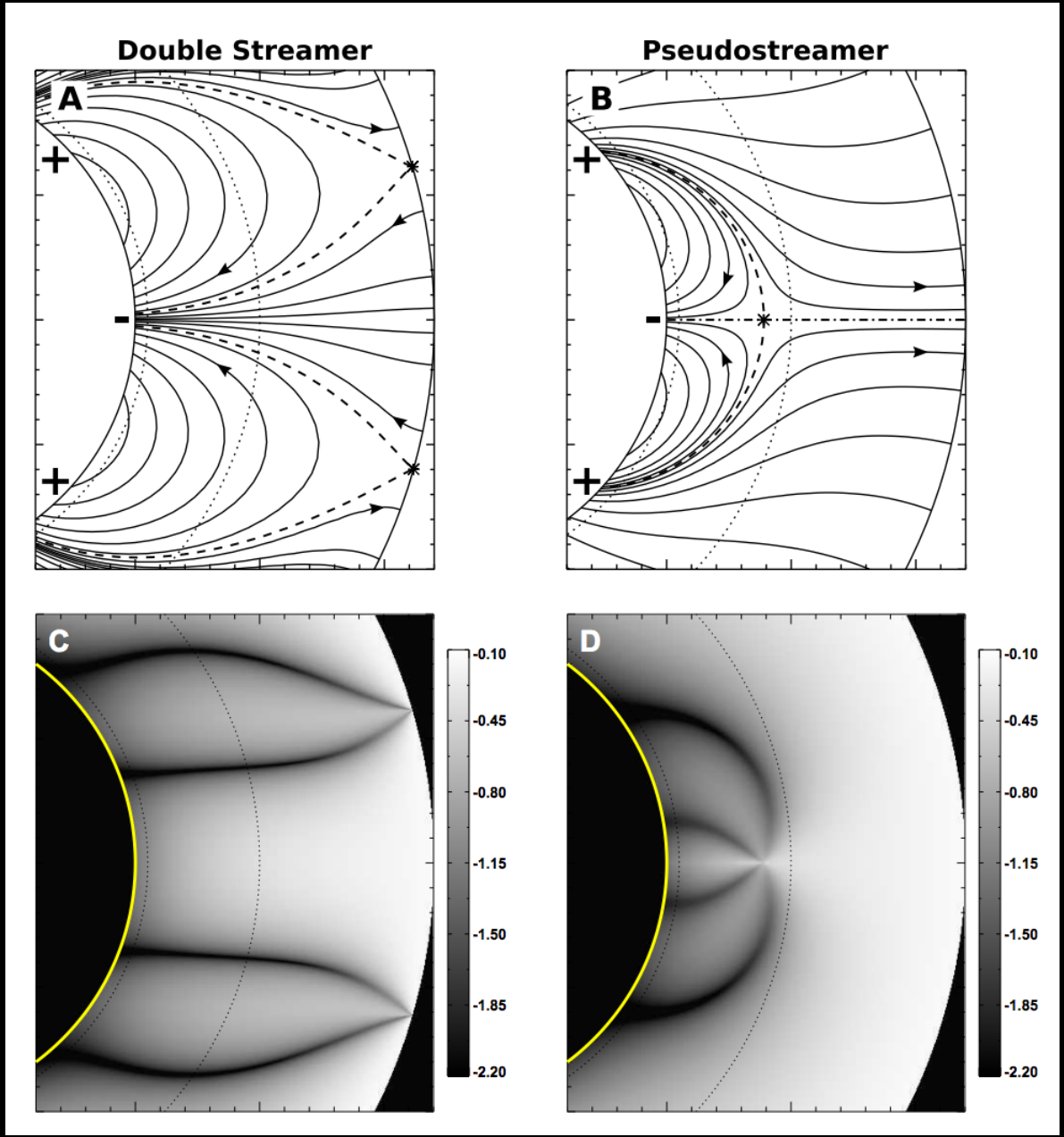

L/I

Rachmeler et al 2014

Pseudostreamers in CoMP linear polarization

Rachmeler et al 2016

CoMP observations

L/I

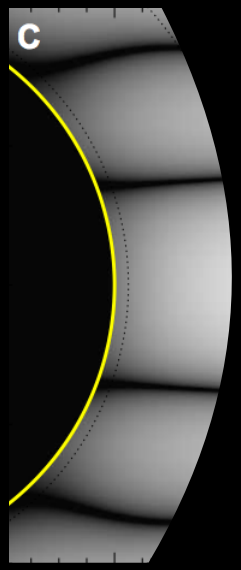

Double Streamer

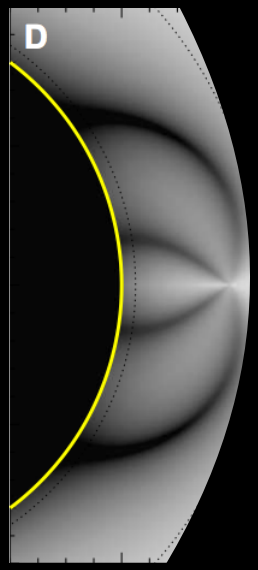

Pseudostreamer

Pseudostreamers in CoMP linear polarization

Rachmeler et al 2016

CoMP observations

LI

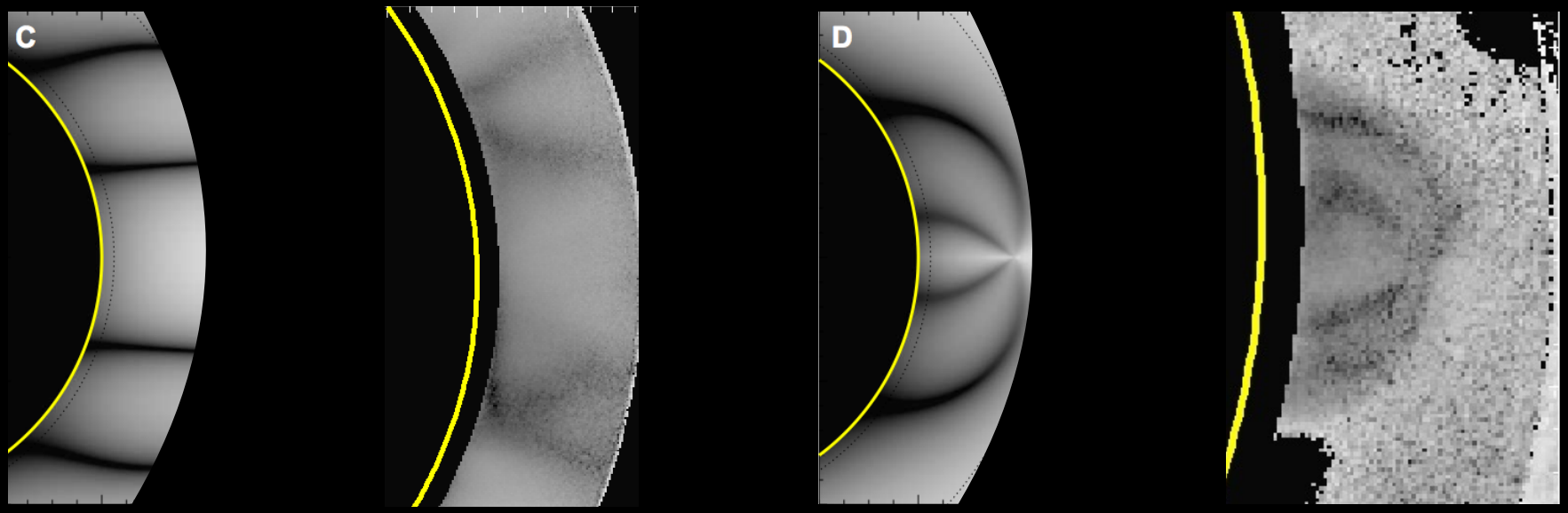

Pseudostreamers and solar cycle variation

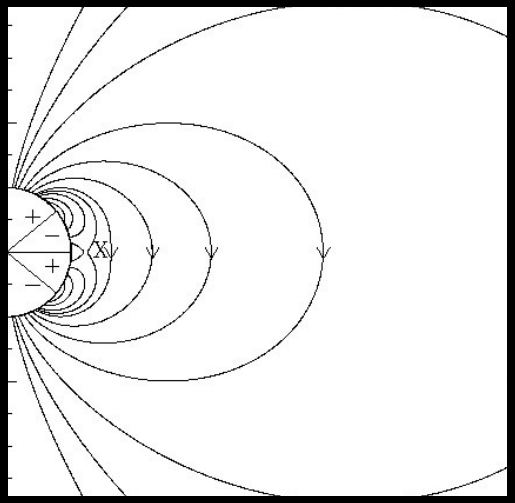

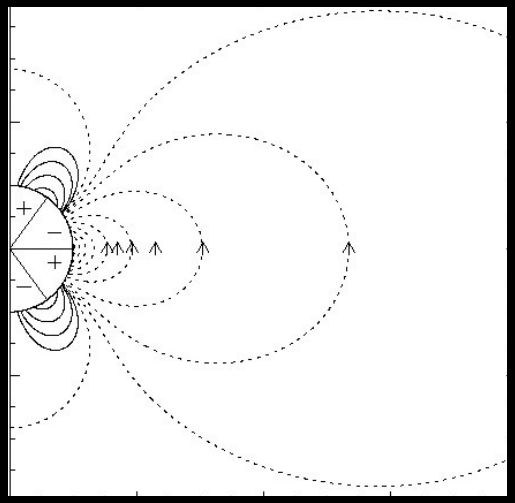

- Solar polar field reverses in response to flux emergence
- Coronal field may reverse before photospheric field

Zhang and Low, 2001

Pseudostreamers and solar cycle variation

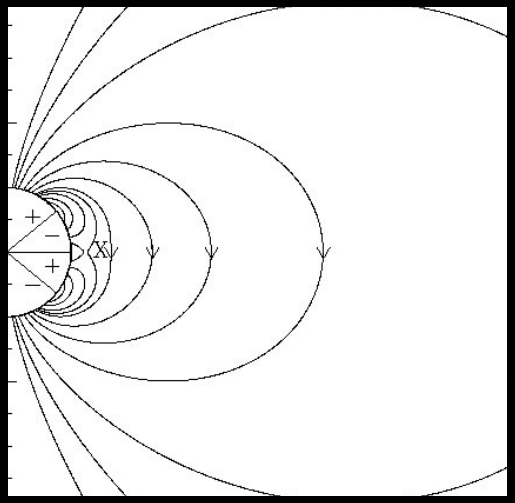

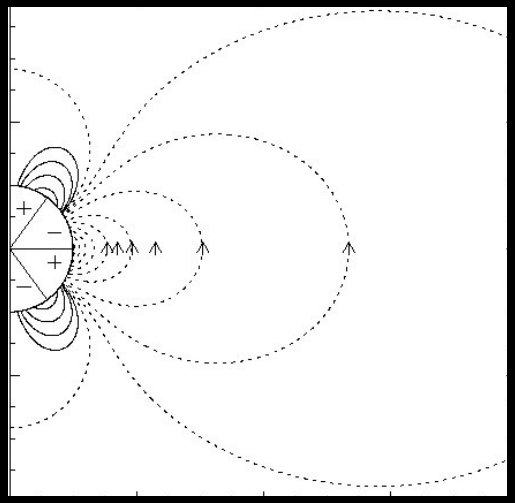

- Solar polar field reverses in response to flux emergence
- Coronal field may reverse before photospheric field

Zhang and Low, 2001

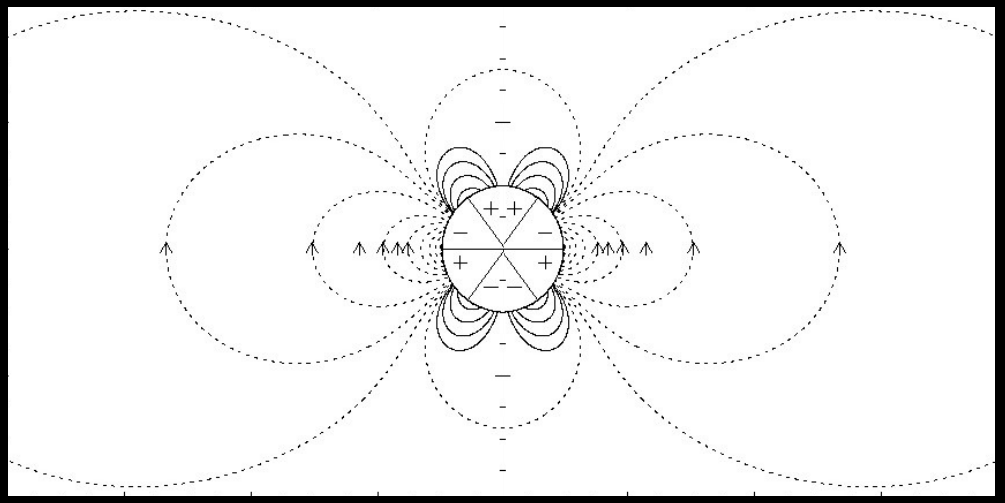

Pseudostreamer at poles

Rachmeler — next talk

Pseudostreamers and solar cycle variation

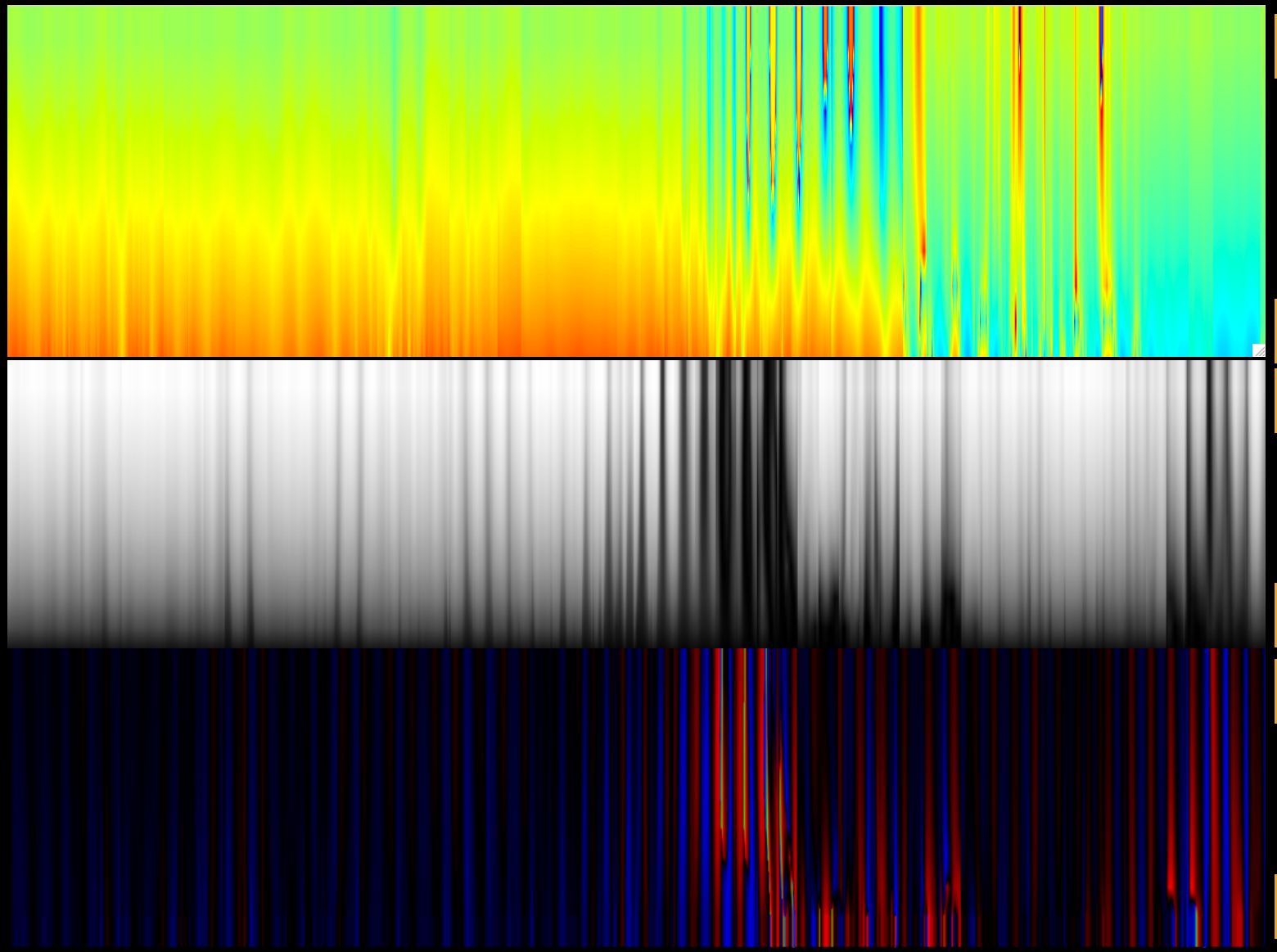

PSI MAS model Carr. rots, 2010 June 1 — 2014 December 31
south pole, +/- 5 degrees lat. average

Pseudostreamers and solar cycle variation

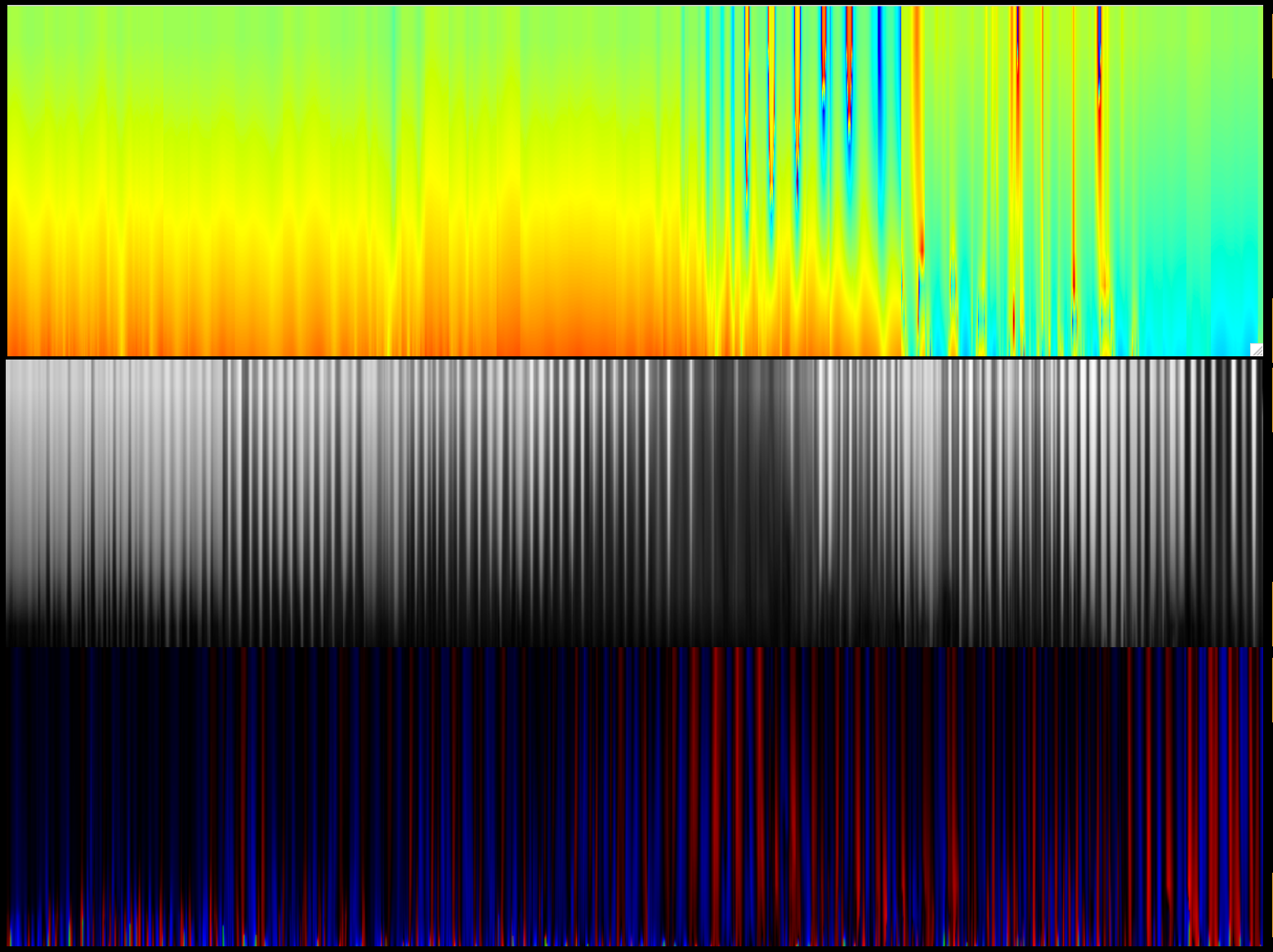

PSI MAS model Carr. rots, 2010 June 1 — 2014 December 31
south pole, +/- 5 degrees lat. average

Non-radial expansion in CoMP

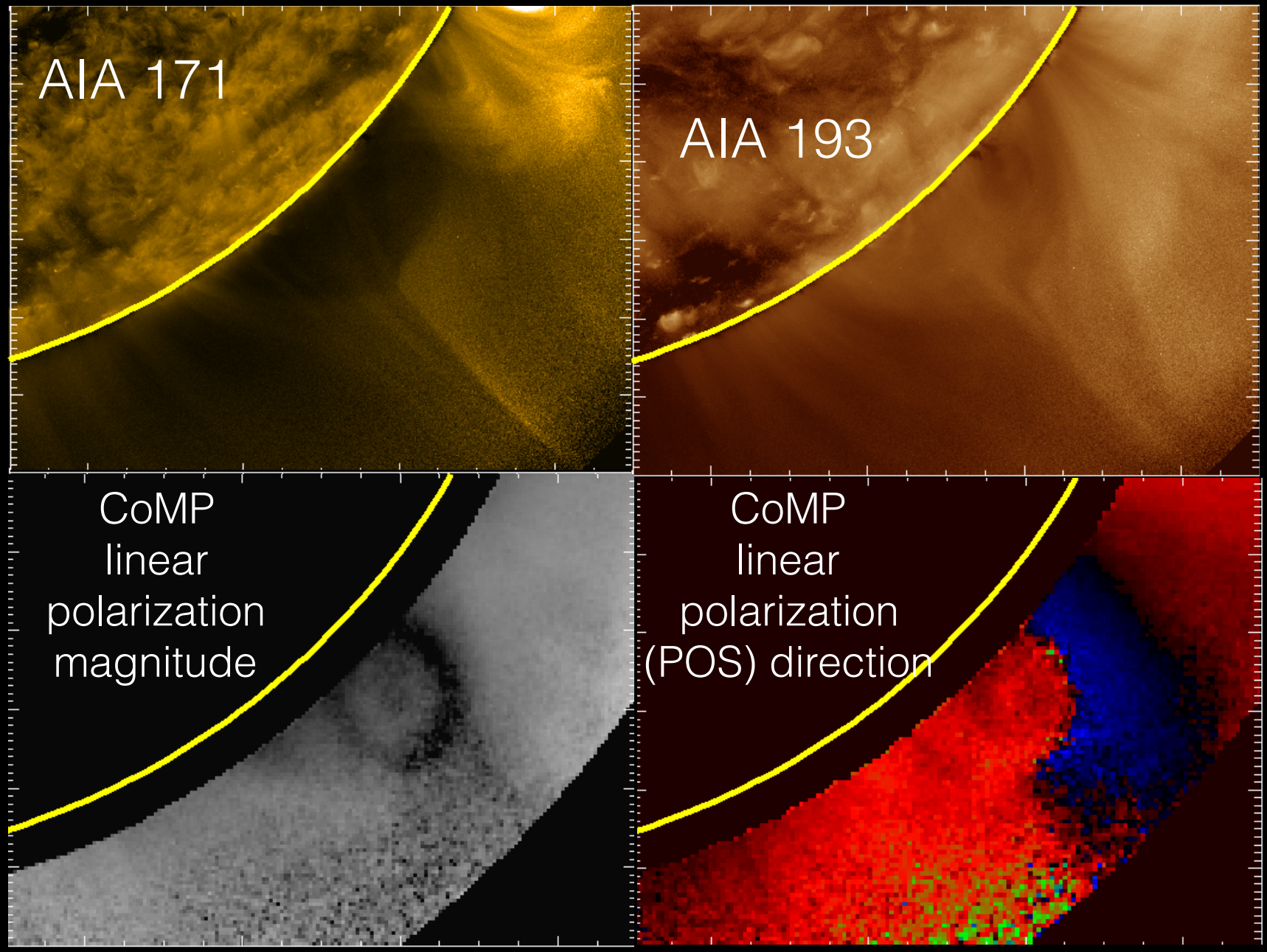

2015 April 18 Pseudostreamer

Non-radial expansion in CoMP

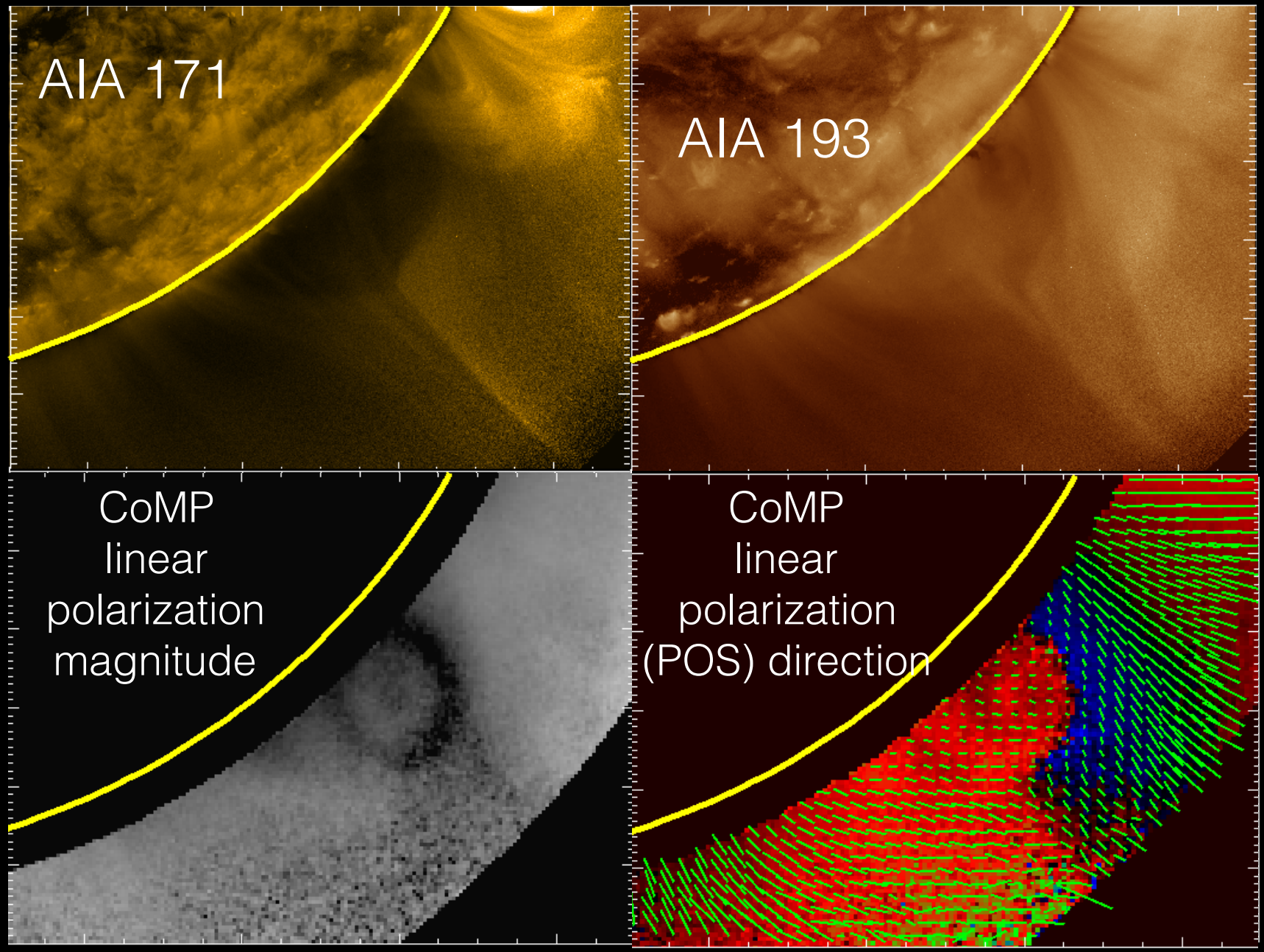

2015 April 18 Pseudostreamer

Non-radial expansion in CoMP

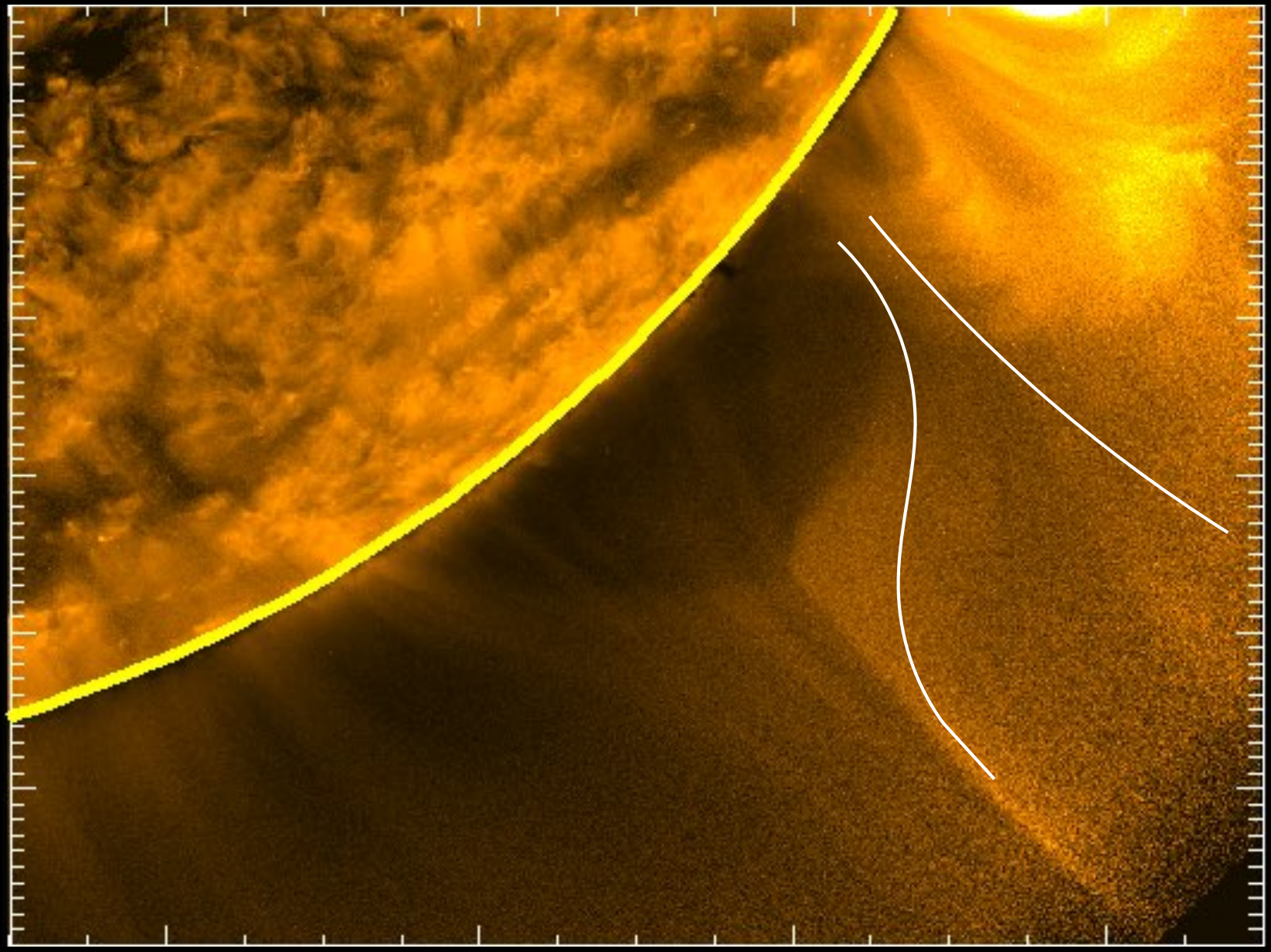

New diagnostic of expansion factor

Non-radial expansion in CoMP

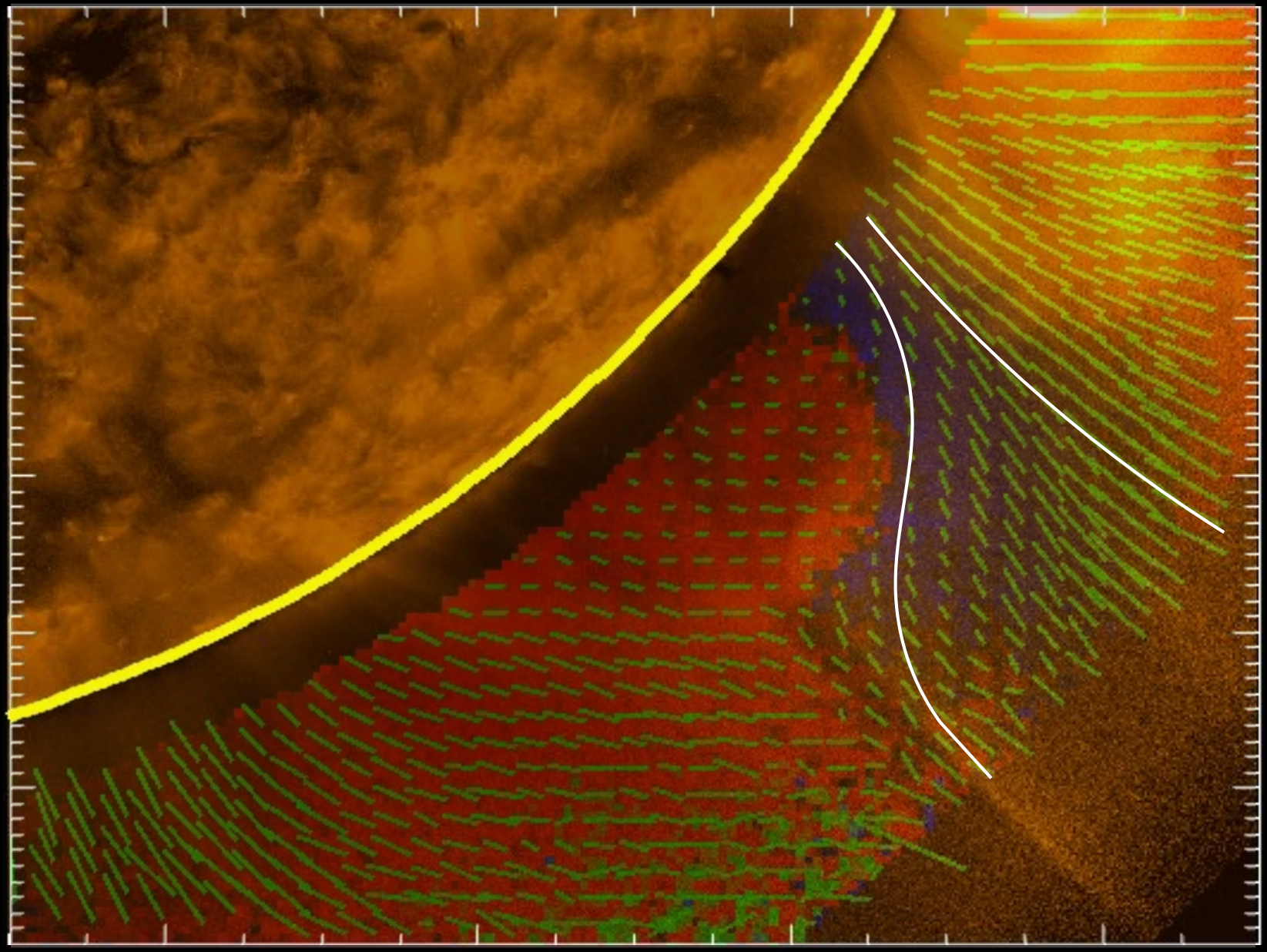

New diagnostic of expansion factor

Non-radial expansion in CoMP

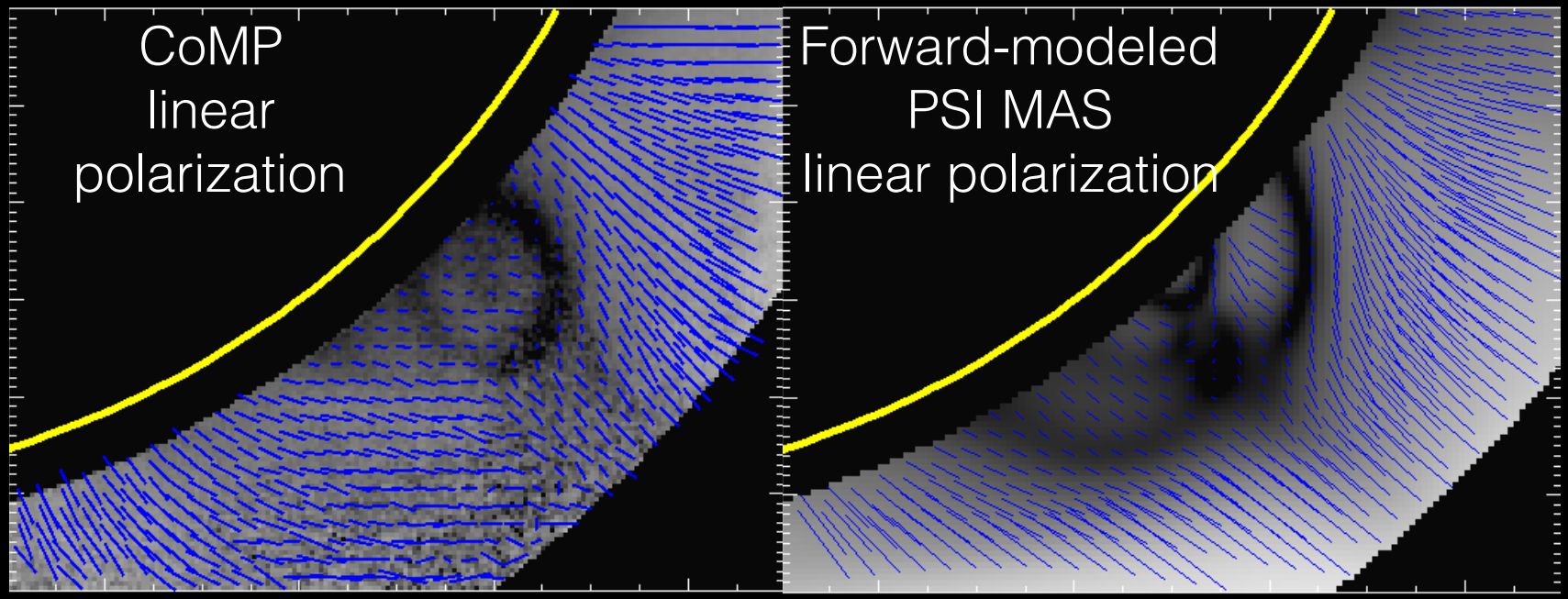

New diagnostic of expansion factor

Non-radial expansion in CoMP

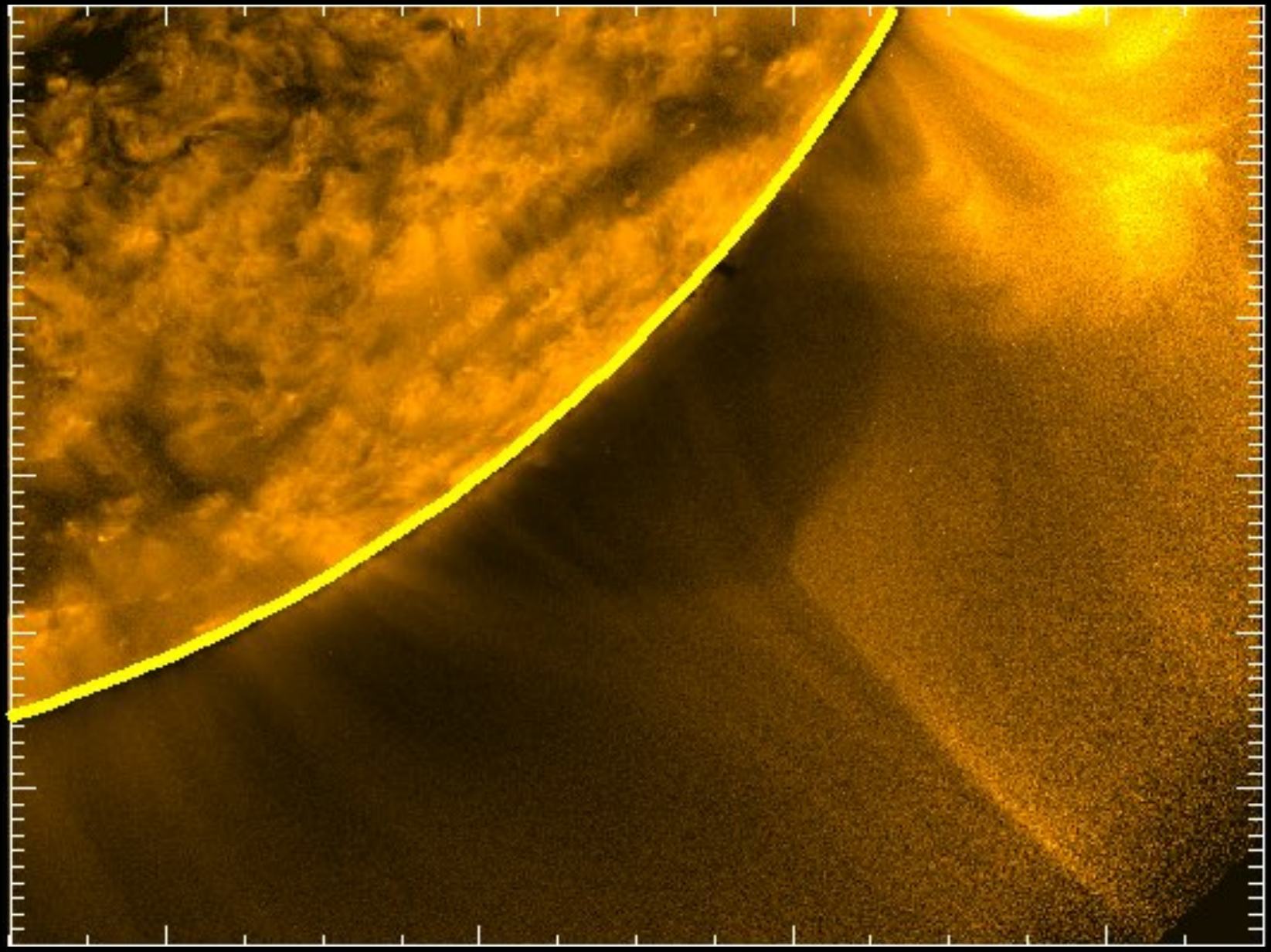

Non-radial expansion in CoMP

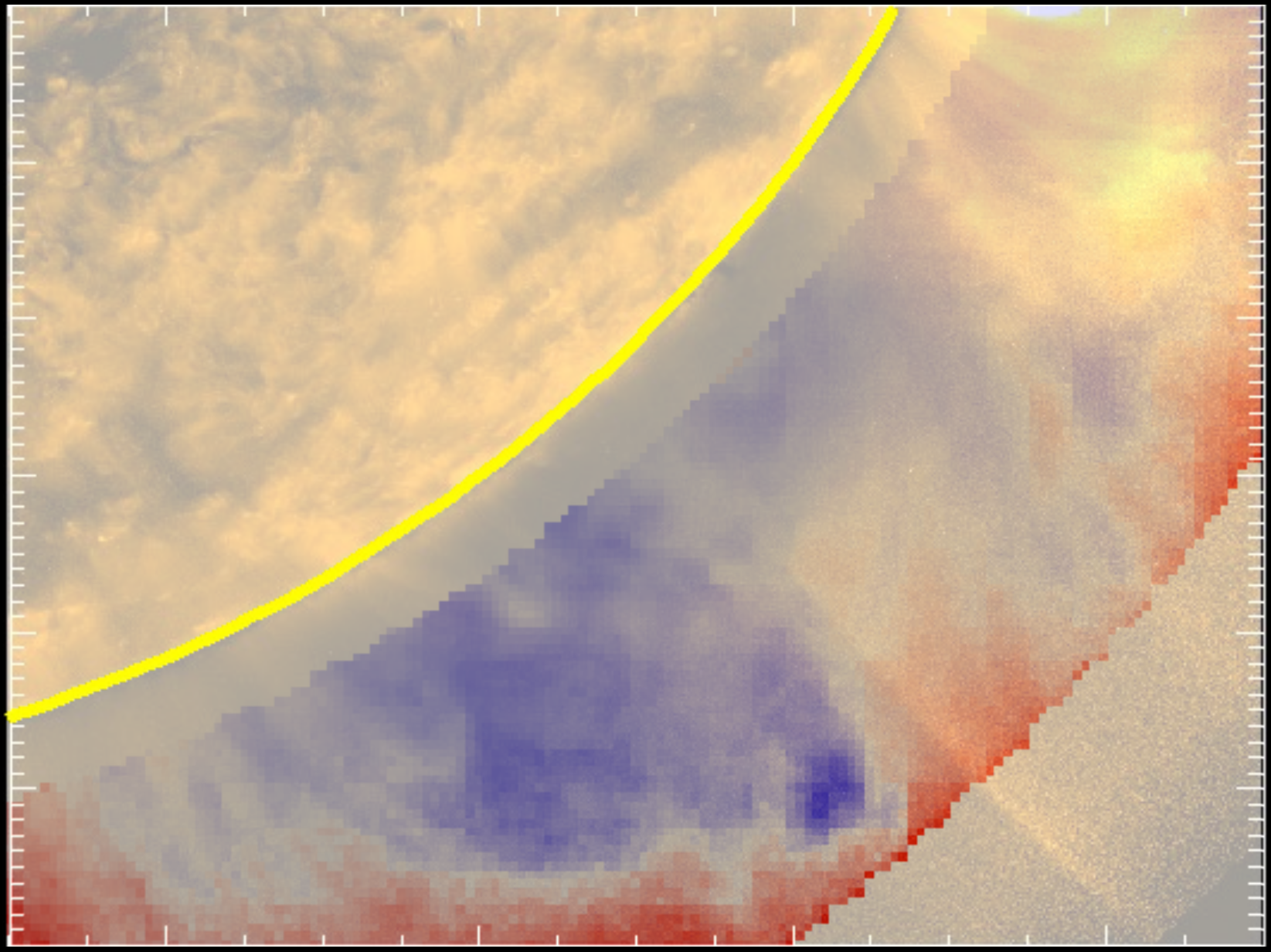

Non-radial expansion in CoMP

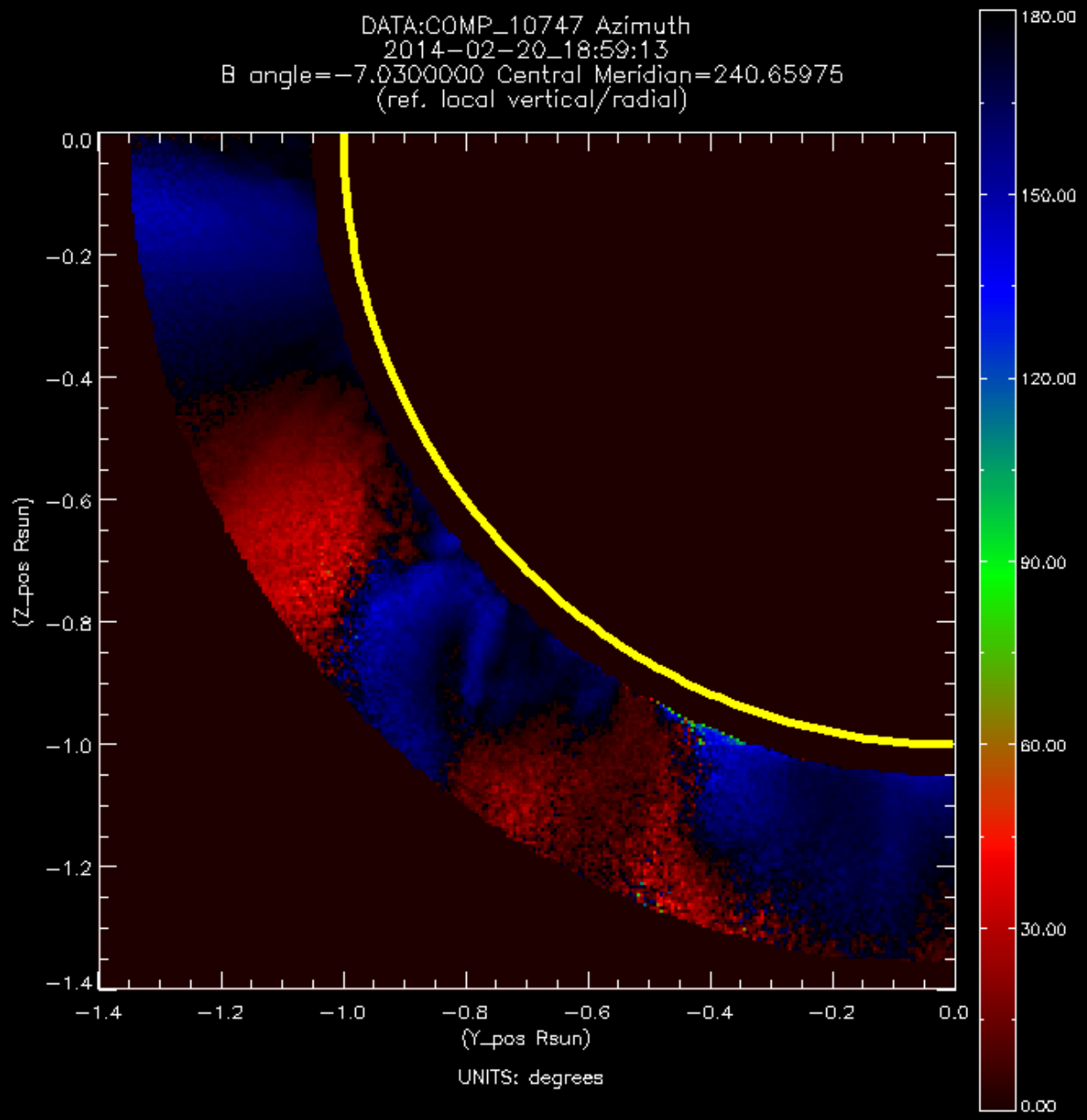

Non-radial expansion in CoMP

diverging fields

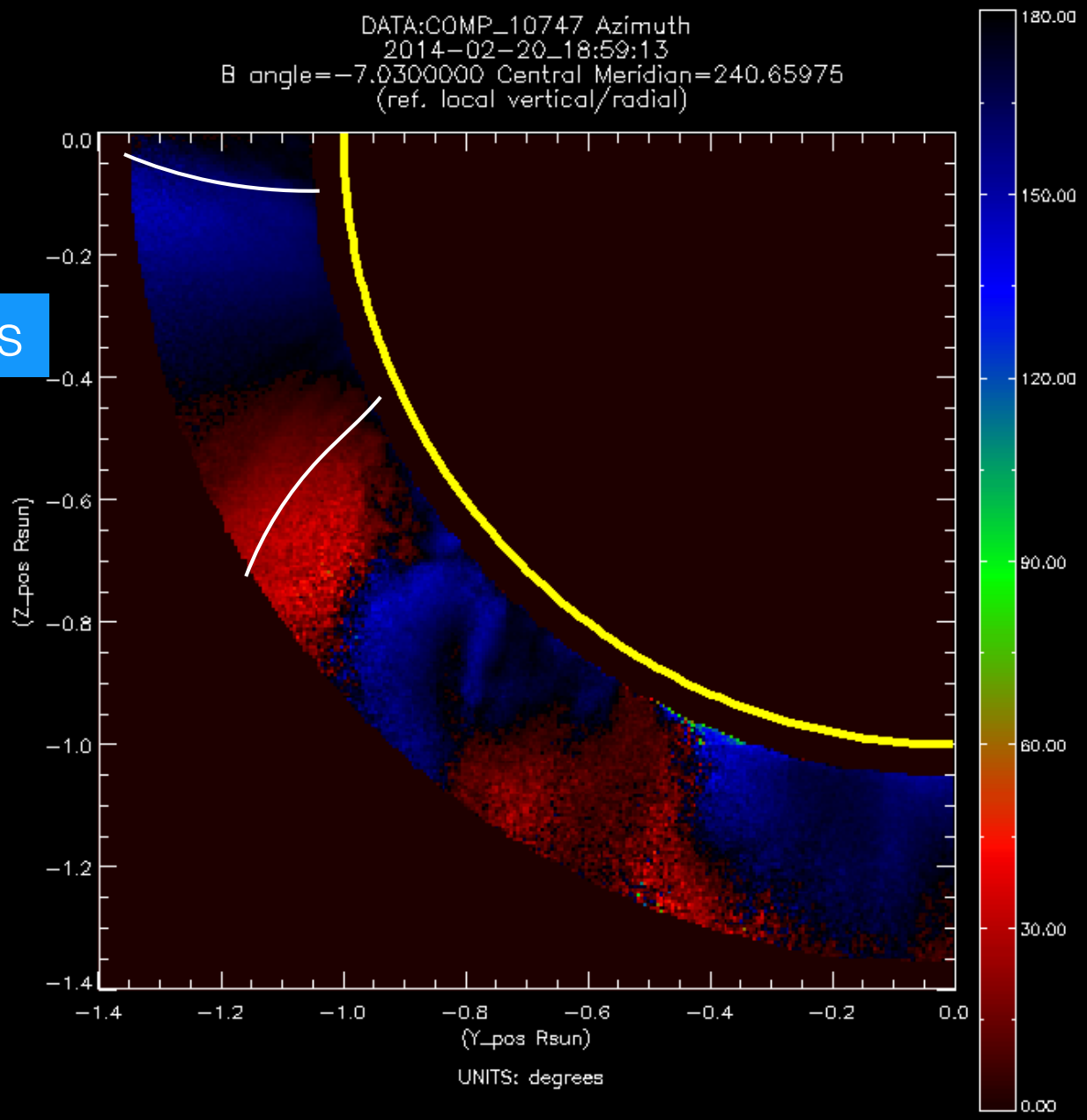

Non-radial expansion in CoMP

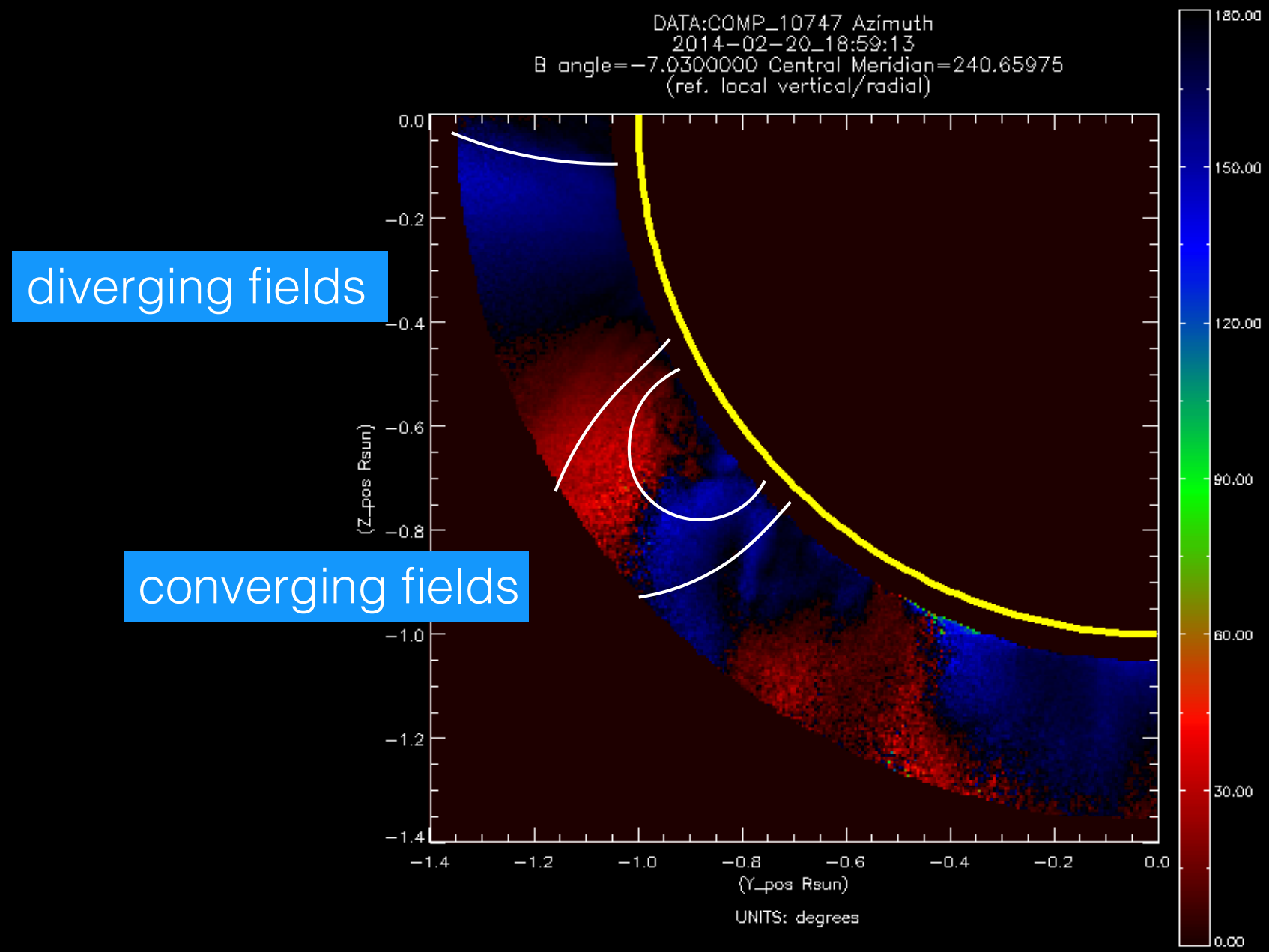

diverging fields

converging fields

Non-radial expansion in CoMP

diverging fields

converging fields

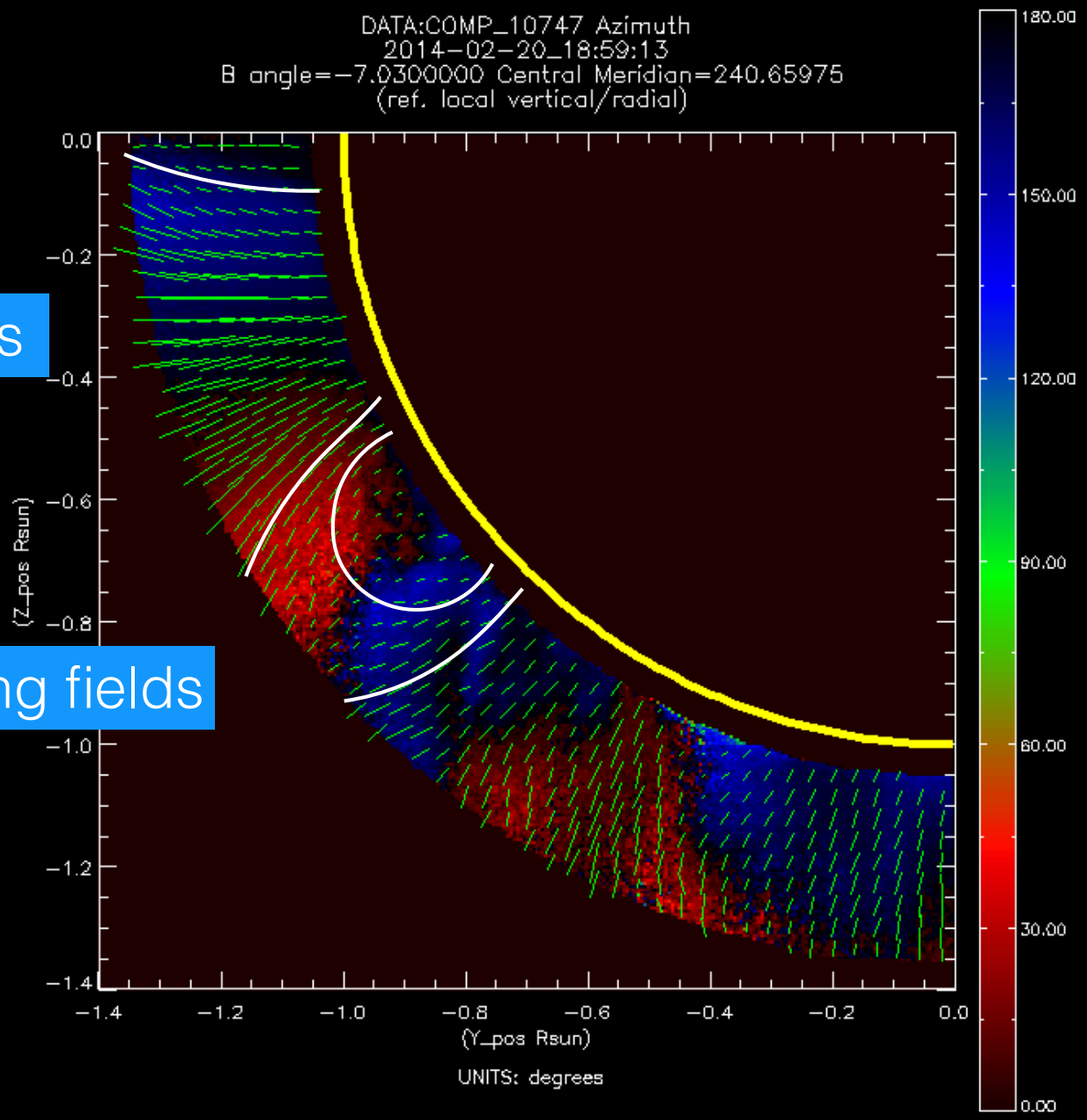

Non-radial expansion in CoMP

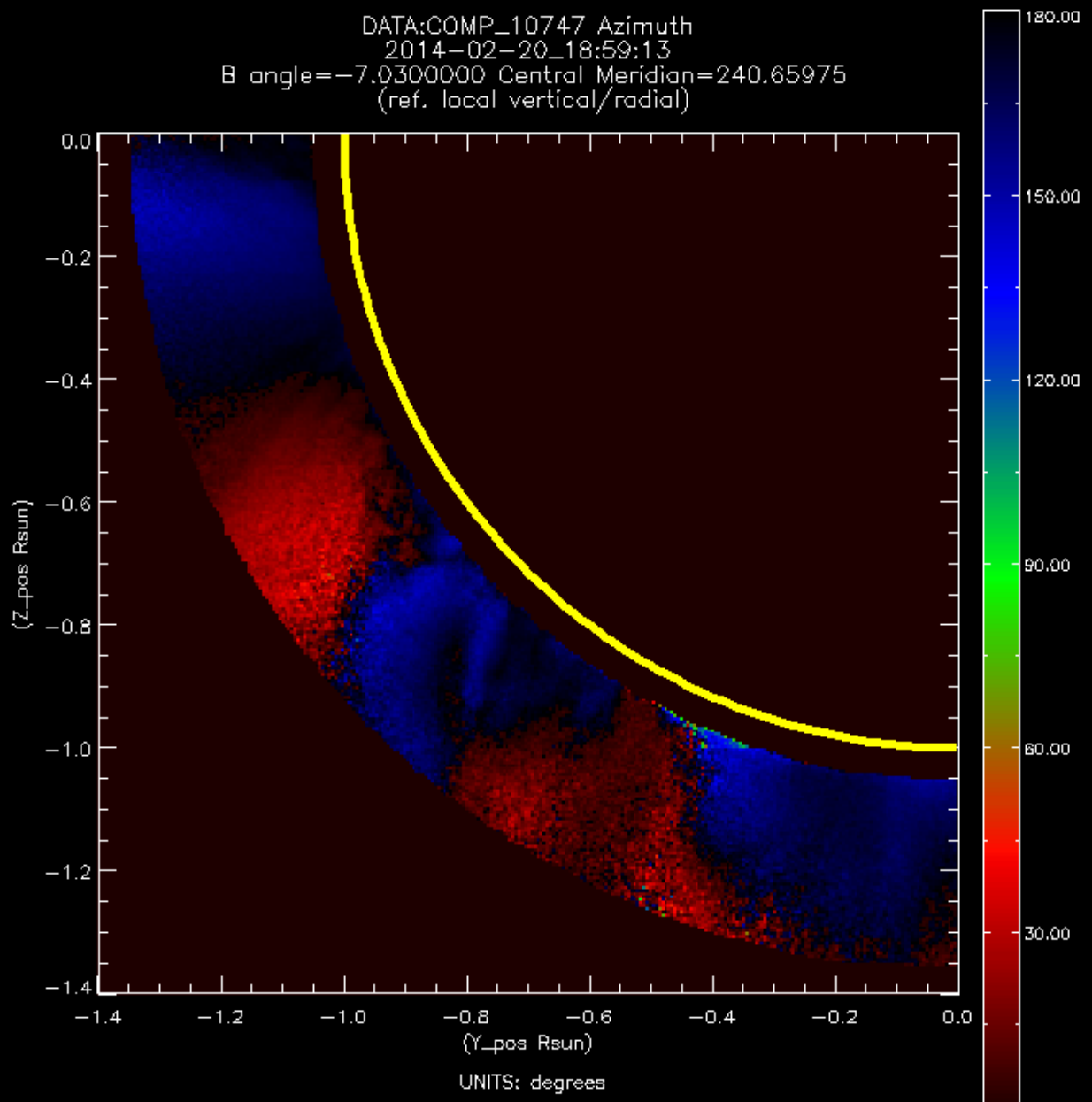

CoMP observations

Non-radial expansion in CoMP

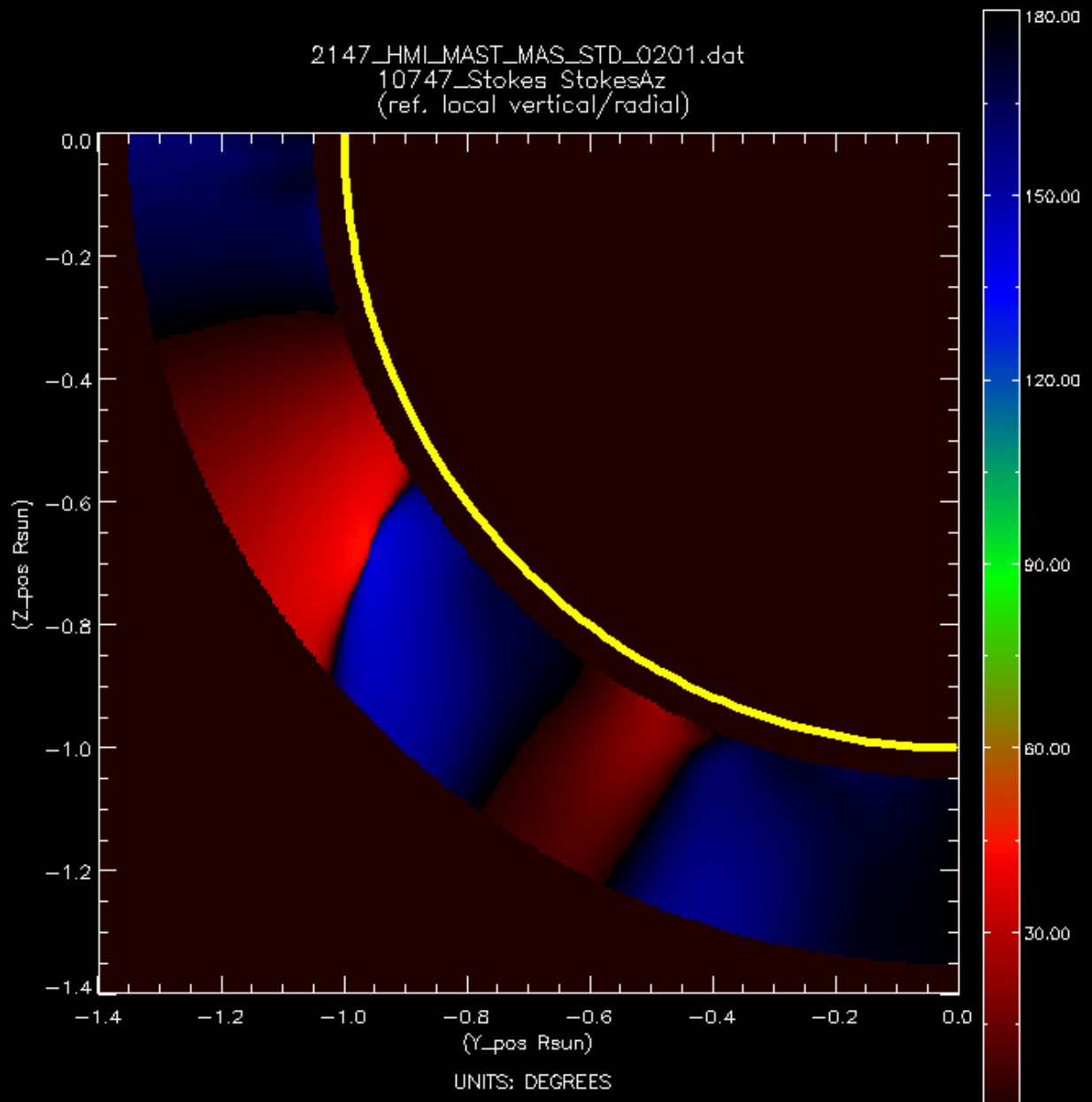

MAS model

Non-radial expansion in CoMP

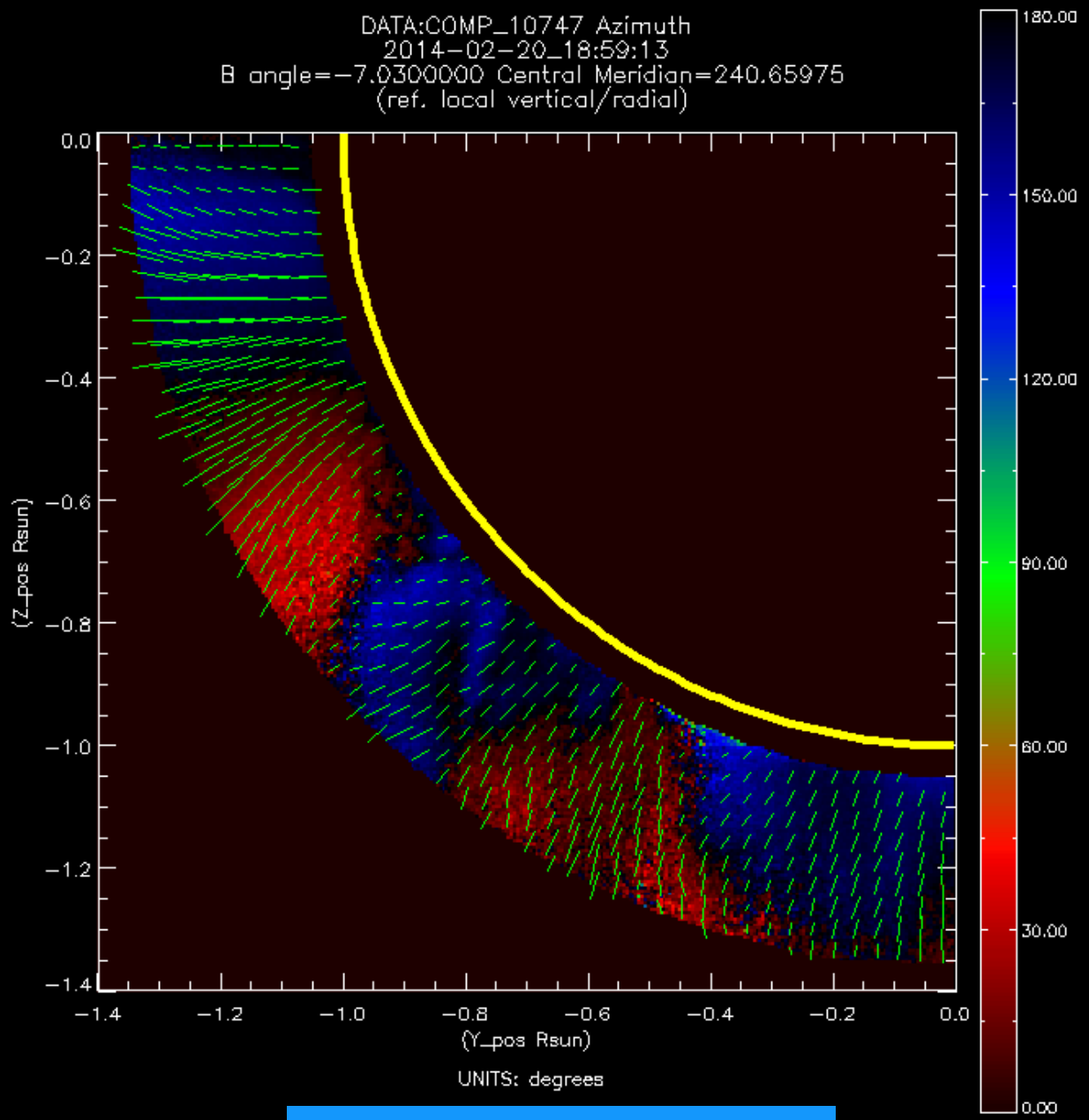

CoMP observations

Non-radial expansion in CoMP

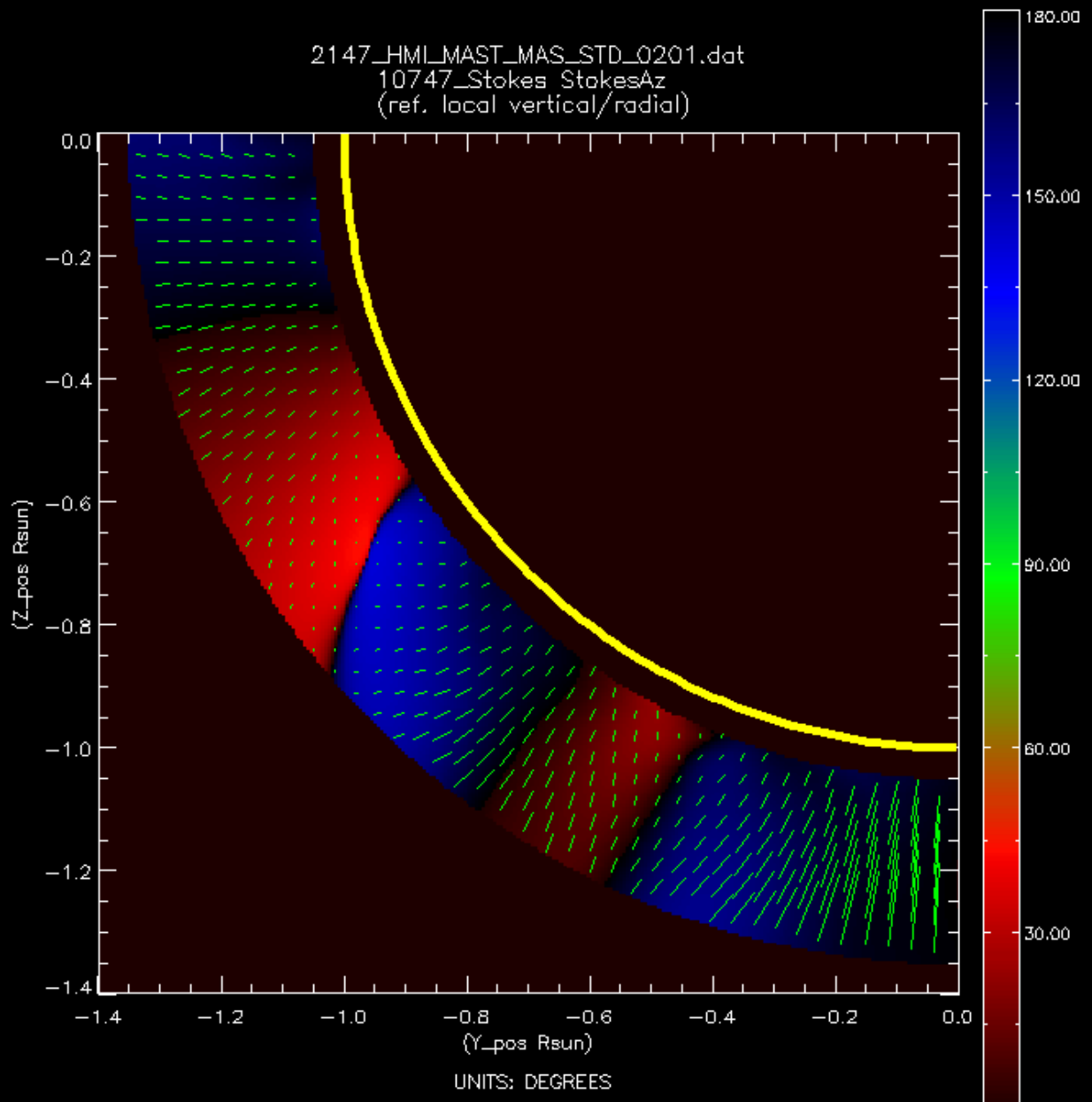

MAS model

Non-radial expansion in CoMP

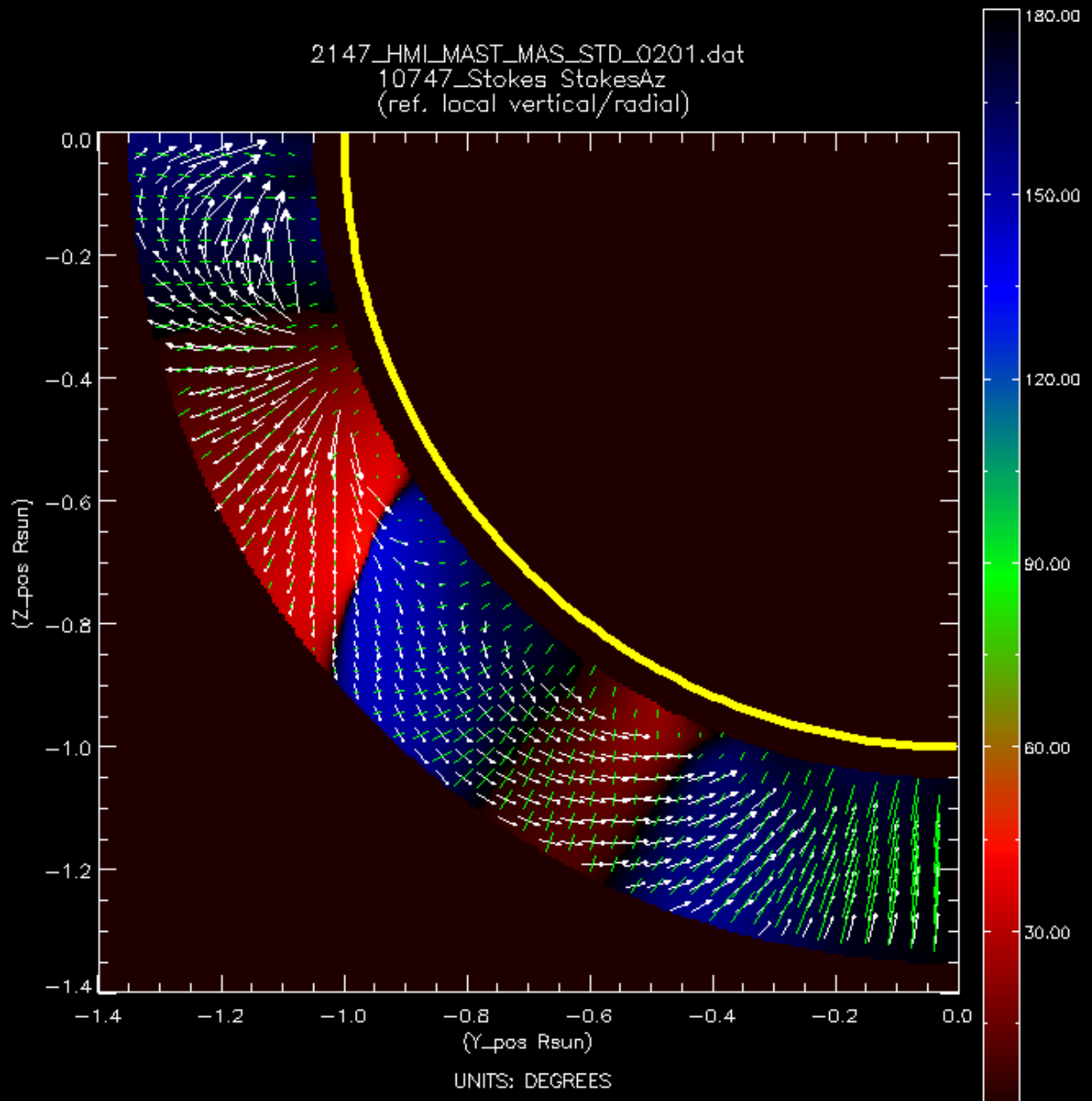

MAS model

Conclusions

CoMP linear polarization data diagnose flux ropes, pseudostreamers, and non-radially expanding fields

Useful for topological studies of all sorts, e.g. targeting solar eruptive stability and solar cycle evolution

New diagnostic of expansion factor: important for model validation and significant to solar-wind analyses

CoMP linear polarization data are a largely-untapped resource, freely available at HAO/MLSO web site along with diagnostic tools (FORWARD)